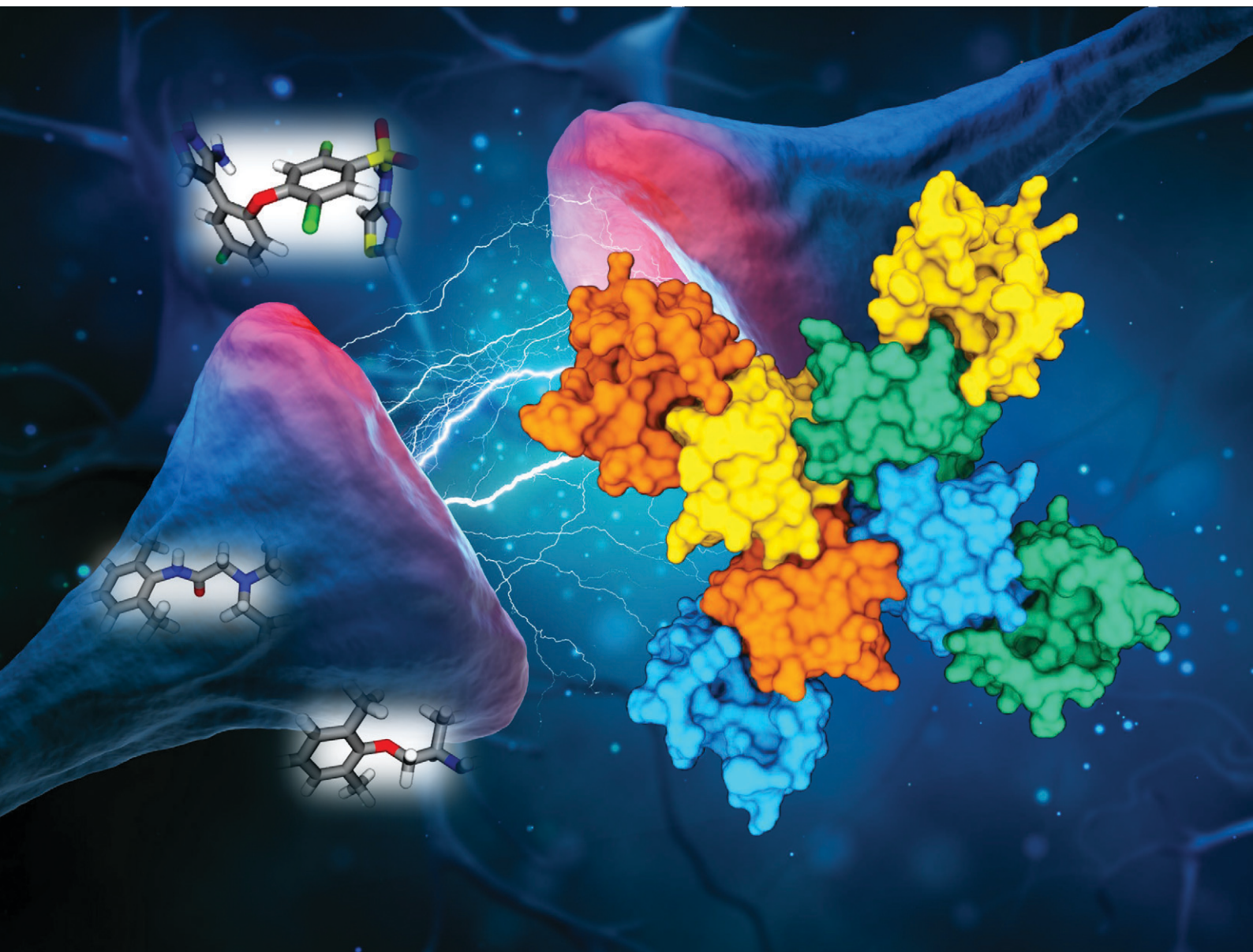


Volume 13
Number 8
August 2022
Pages 887-1000

RSC Medicinal Chemistry

rsc.li/medchem



ISSN 2632-8682

REVIEW ARTICLE

Yutaka Kitano and Tsuyoshi Shinozuka
Inhibition of Na_v1.7: the possibility of ideal analgesics

REVIEW



Cite this: *RSC Med. Chem.*, 2022, 13, 895

Received 9th March 2022,
Accepted 25th July 2022

DOI: 10.1039/d2md00081d

rsc.li/medchem

Inhibition of Na_v1.7: the possibility of ideal analgesics†

Yutaka Kitano and Tsuyoshi Shinozuka *

The selective inhibition of Na_v1.7 is a promising strategy for developing novel analgesic agents with fewer adverse effects. Although the potent selective inhibition of Na_v1.7 has been recently achieved, multiple Na_v1.7 inhibitors failed in clinical development. In this review, the relationship between preclinical *in vivo* efficacy and Na_v1.7 coverage among three types of voltage-gated sodium channel (VGSC) inhibitors, namely conventional VGSC inhibitors, sulphonamides and acyl sulphonamides, is discussed. By demonstrating the PK/PD discrepancy of preclinical studies *versus in vivo* models and clinical results, the potential reasons behind the disconnect between preclinical results and clinical outcomes are discussed together with strategies for developing ideal analgesic agents.

1. Introduction

Pain sensation is a critical signal for preventing dangerous signs, and consecutive instances of pain are often problematic. Chronic pain is one of the most typical symptoms reported by patients, and it sometimes has devastating consequences, resulting in a huge economic burden on the health care system.¹ To alleviate such devastating conditions, various analgesic agents are utilised in clinical settings.^{2–6} Typical analgesic agents are listed in Table 1. Opioids are highly efficacious agents for the treatment of pain disorders, but their abuse potential is a critical concern.⁴ Although non-steroidal anti-inflammatory drugs (NSAIDs) are useful for treating inflammatory pain, their maximum efficacy and duration of efficacy are limited. It was reported that the prolonged use of NSAIDs was associated with gastrointestinal (GI) and cardiovascular (CV) adverse effects.⁵ Gabapentinoids are specific ligands for the $\alpha_2\delta$ subunit of voltage-gated Ca²⁺ channels, and they are widely used in the first-line treatment of neuropathic pain (NP). However, central nervous system (CNS) adverse effects such as dizziness, somnolence or abuse potential, together with narrow safety margins, should be considered in the use of gabapentinoids.⁶ Although voltage-gated sodium channel (VGSC, Na_v) inhibitors are also efficacious for various pain disorders, CNS and CV adverse effects often limit their usage.⁷ Thus, the unmet medical needs in the treatment of pain disorders remain considerably high, and many analgesic drug candidates have been extensively developed.^{2,3}

VGSCs regulate neuronal signals in the CNS and peripheral nervous system (PNS). Since the discovery of such fundamental roles of VGSCs, their modulation has been studied extensively for the treatment of various disorders, including epilepsy and pain. In 2006, the discovery of loss-of-function mutations of the Na_v1.7 gene (SCN9A) in humans accelerated such efforts. A hereditary loss-of-function mutation of SCN9A leads to a rare genetic condition called congenital insensitivity to pain (CIP), which is characterised by the inability to perceive physical pain.⁸ Although patients with CIP exhibit a normal phenotype similar to that of healthy individuals, they experience anosmia, which is a lack of olfactory function.⁹ Conversely, the excessive expression of SCN9A leads to hereditary pain disorders, such as paroxysmal extreme pain disorder (PEPD) and inherited erythromelalgia (IEM).¹⁰ Gain-of-function variants of SCN9A are also associated with itch conditions in humans.¹¹ The fundamental role in pain signalling by Na_v1.7 has been reported in rodents. Although global deletion of SCN9A is

Table 1 The targets for analgesics

Target	Target location	Example	Challenges
Opioid	CNS	Morphine Fentanyl	Abuse potential
Inhibition of prostaglandin synthesis (NSAID)	Peripheral tissue	Aspirin Diclofenac Loxoprofen	Limited efficacy GI and CV adverse effects
Gabapentinoid ($\alpha_2\delta$ ligand)	CNS	Gabapentin Pregabalin Mirogabalin	CNS adverse effects
VGSC inhibitor	PNS and CNS	Lidocaine Mexiletine	CNS and CV adverse effects

R&D Division, Daiichi Sankyo Co., Ltd., 1-2-58 Hiromachi, Shinagawa-ku, Tokyo 140-8710, Japan. E-mail: sinozu.xf6@gmail.com, shinozuka.tsuyoshi.s5@daiichisankyo.co.jp

† Electronic supplementary information (ESI) available. See DOI: <https://doi.org/10.1039/d2md00081d>

lethal in mice, genetic and animal husbandry approaches enabled the construction of global¹² and conditional¹³ $\text{Na}_v1.7$ knockout mice, the phenotype of which was analogous to the pain-free phenotype observed in patients with CIP: anatomically normal with complete insensitivity to painful mechanical, thermal and chemical stimuli. In conditional $\text{Na}_v1.7$ knockout mice, the deletion of SCN9A in both sensory and sympathetic neurons was required for generating the same phenotype observed in humans even though $\text{Na}_v1.7$ is mainly expressed in the PNS.¹³ Although both global and conditional knockout mice display anosmia,^{9,12} conditional knockout rats retain olfactory function with a pain-free phenotype.¹⁴ The epigenome engineering approach that utilised CRISPER-dCas and zinc finger proteins to ablate the expression of $\text{Na}_v1.7$ in mice led to long-lasting analgesic efficacy. In some cases, the analgesic effect lasted for up to 44 weeks.¹⁵ This genetic evidence clearly and strongly demonstrates that $\text{Na}_v1.7$ inhibition is a promising therapeutic approach for developing analgesic agents with fewer adverse effects.

The VGSC family consists of nine subtypes ($\text{Na}_v1.1$ – $\text{Na}_v1.9$, Table 2) with a variety of reported roles.¹⁶ The VGSC family is classified by sensitivity to the neurotoxin tetrodotoxin (TTX); specifically, the functions of $\text{Na}_v1.1$ – $\text{Na}_v1.4$, $\text{Na}_v1.6$ and $\text{Na}_v1.7$ are inhibited by TTX, whereas $\text{Na}_v1.5$, $\text{Na}_v1.8$ and $\text{Na}_v1.9$ are TTX-resistant. $\text{Na}_v1.1$ and $\text{Na}_v1.2$ are mainly expressed in the CNS, and mutation studies revealed that both neuronal sodium channels are associated with epilepsy.¹⁷ Although $\text{Na}_v1.3$ is mainly expressed in the embryonic stage, the up-regulation of SCN3A was reported in inflammatory or NP conditions.¹⁸ $\text{Na}_v1.5$ is highly expressed in cardiac muscle, and SCN5A mutations cause primarily inherited cardiomyopathies, including congenital long QT syndrome type 3 and Brugada syndrome.¹⁹ $\text{Na}_v1.7$ is preferentially expressed in dorsal root ganglion (DRG) and sympathetic neurons in the PNS, and its expression in olfactory sensory neurons was reported.²⁰ Given the distribution of $\text{Na}_v1.7$, its selective inhibition is a promising strategy for novel analgesics with superior safety profiles and fewer CNS and CV adverse effects. $\text{Na}_v1.8$ is highly expressed in the DRG, and the ablation of SCN10A in rodents led to deficits in nociception. As gain-of-function mutations of SCN10A result in painful peripheral neuropathy in humans,²¹ $\text{Na}_v1.8$ is a therapeutic target for analgesics. In

fact, selective $\text{Na}_v1.8$ inhibitors displayed efficacy in rodent models of NP.^{22,23} However, $\text{Na}_v1.8$ expression in cardiac muscle is considered to be a potential risk associated with CV side effects and a drawback compared to $\text{Na}_v1.7$.²⁴

Two fibres, specifically A δ - and C-fibres, play predominant roles in the transaction of pain signals in the PNS (Table 3). When peripheral sensory neurons, termed nociceptors, in the DRG receive a nociceptive pain sensation, they transmit the sensation as electrical impulses to the CNS *via* the spinal cord, where it synapses onto neurons in the dorsal horn. In the DRG, two small-to-medium-diameter nociceptors, termed myelinated A δ -fibres and unmyelinated C-fibres, transduce nociceptive pain sensation with a high threshold, whereas A α - and A β -fibres, which are large-diameter myelinated fibres, detect innocuous stimuli without contributing to pain signalling.²⁵ A δ -fibres rapidly transmit signals from the PNS to the CNS *via* the spinal cord, known as “first pain” in response to a stimulus, whereas C-fibres transduce “second pain” that is more diffuse and dull and that is perceived with a temporal delay relative to the inciting stimulus.

Although genetic evidence strongly suggests that selective inhibition of $\text{Na}_v1.7$ is a promising analgesic approach, the structural similarity of VGSC family members has hampered this strategy. A pore-forming α subunit and a stabilising β subunit comprise the backbone of VGSCs, and they exhibit high amino acid sequence homology in the extracellular and transmembrane domains.²⁶ Conventional $\text{Na}_v1.7$ inhibitors are less subtype-selective with inhibitory potency in the micromolar range. In 2010, Pfizer disclosed a highly potent selective $\text{Na}_v1.7$ inhibitor in their patent.²⁷ This fuelled the development of a new generation of highly potent selective $\text{Na}_v1.7$ inhibitors for the potential treatment of pain disorders, and inevitably, many pharmaceuticals and biotech firms initiated research and development on aryl sulphonamide derivatives followed by the disclosure of potent selective $\text{Na}_v1.7$ inhibitors in patents or papers. Although many highly potent selective $\text{Na}_v1.7$ inhibitors have been disclosed and some of them have been examined for their analgesic potency in clinical trials, none has reached the market.

In this article, we review conventional $\text{Na}_v1.7$ inhibitors, some of which have been successfully launched into the market. Then, the highly potent selective sulphonamide and acyl sulphonamide derivatives are reviewed. By demonstrating the PK/PD discrepancy of preclinical studies relative to *in vivo* models and clinical results, we discuss potential reasons behind the disconnect between preclinical results and clinical outcomes and strategies for developing ideal analgesic agents.

Table 2 VGSC family

Subtype	Gene	TTX sensitivity	Major expression sites
$\text{Na}_v1.1$	SCN1A	Sensitive	PNS, CNS
$\text{Na}_v1.2$	SCN2A	Sensitive	CNS
$\text{Na}_v1.3$	SCN3A	Sensitive	PNS, CNS (embryonic)
$\text{Na}_v1.4$	SCN4A	Sensitive	Skeletal muscle
$\text{Na}_v1.5$	SCN5A	Resistant	Cardiac muscle
$\text{Na}_v1.6$	SCN8A	Sensitive	PNS, CNS
$\text{Na}_v1.7$	SCN9A	Sensitive	PNS
$\text{Na}_v1.8$	SCN10A	Resistant	PNS, cardiac muscle
$\text{Na}_v1.9$	SCN11A	Resistant	PNS

Table 3 Fibres in the PNS

Fibre	Diameter	Myelinated	Nociceptor
A α - and A β -fibres	Large	Myelinated	Proprioception
A δ -fibre	Medium	Lightly myelinated	Nociception
C-fibre	Small	Unmyelinated	Nociception

2. Structure of VGSC

After the first crystal structure of VGSC from *Arcobacter butzleri* was reported in 2011,²⁸ the crystal structure of Na_v1.7 bound to sulphonamide derivative²⁹ and the cryo-electron microscopy structures of human Na_v1.7 with its auxiliary β subunit bound to TTX or saxitoxin (STX)³⁰ were disclosed. These studies contributed to clarification of the whole structure of Na_v1.7 with the detailed binding mode of such VGSC inhibitors.³¹

VGSC consists of a pore-forming α-subunit and a β-subunit. The α-subunit plays a significant role in channel function, whereas the β-subunit is a multifunctional signalling molecule that also regulates sodium ion conductance. Although the majority of channelopathies including CIP, PEPD and IEM are caused by mutations in the α-subunit, it was also reported that mutations in genes encoding the β-subunit lead to various channelopathies.³²

The α-subunit consists of four domains (DI–DIV), each of which features six α-helical transmembrane segments designated S1–S6 (Fig. 1A and B). S1–S4 helical

segments form a voltage-sensing domain (VSD), which is responsible for sensing the charge in the cell membrane. In particular, positively charged S4 helices contribute to regulating the state of VGSC by their movement. The pore domain (PD) is connected to each VSD, comprising S5–S6 segments and extracellular linkers (P-loop), which enables sodium ion conductance in an ion-selective manner.

At least nine binding sites of VGSC are known, as presented in Table 4 and Fig. 1C and D. This section briefly reviews each binding site and the resulting pharmacological effects because such binding sites have been extensively reviewed.³¹

Binding site 1

Neurotoxins including TTX and STX inhibit VGSCs through binding site 1. Binding site 1 is localized to the extracellular region in the pore loop, in proximity to the ion selectivity filter. Neurotoxins bind directly to extracellular pore to inhibit sodium ion inward flow.³⁰

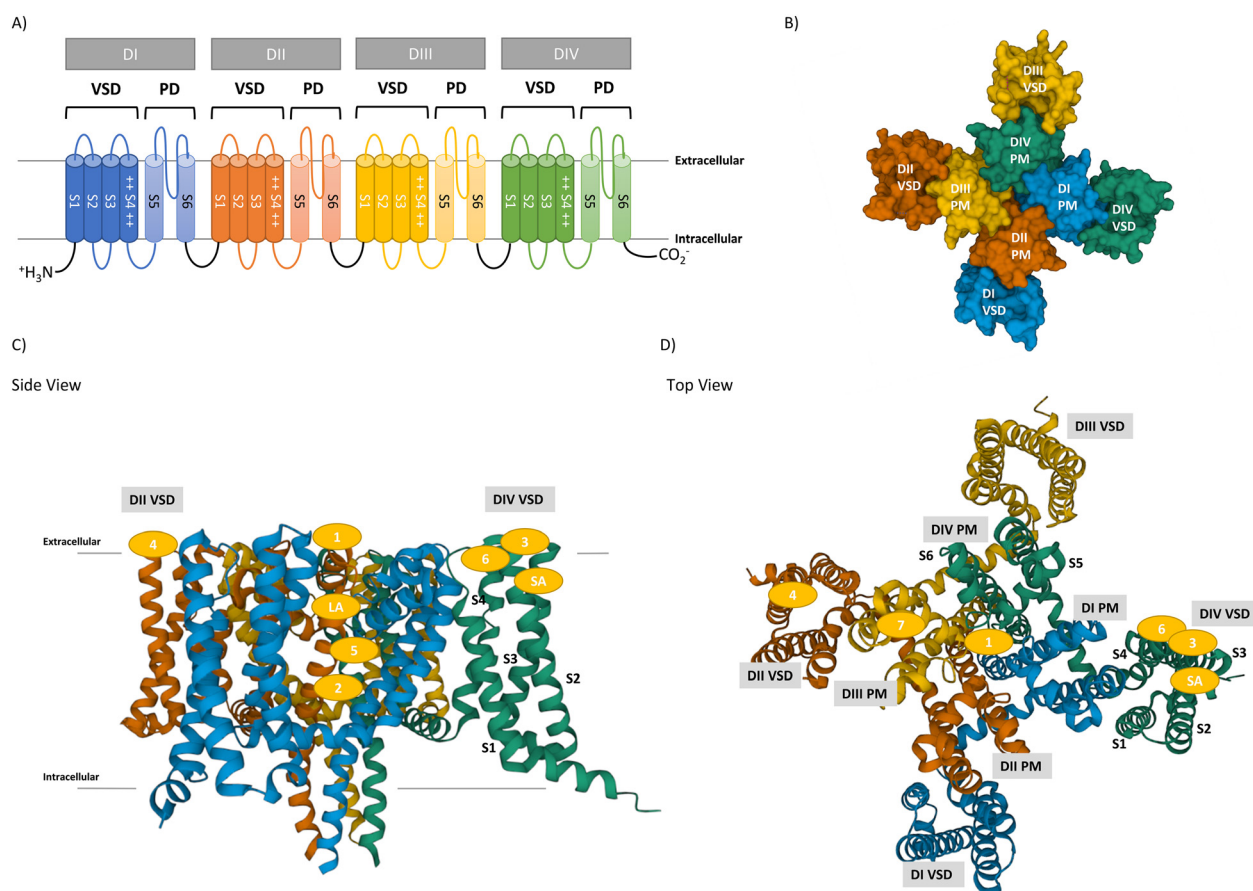


Fig. 1 The structure of VGSC. A) The topology of VGSC pore-forming α subunit. There are six α-helices (S1–S6) in each domain (DI–DIV). Two helices (S5–S6) form the channel pore, and four helices (S1–S4) form a voltage sensor, in which positively charged residues present in each S4 contribute to the conformational change of VGSC *via* membrane voltage. B) Top view of hNav1.7 pore-forming α-subunit with its domains presented in a space-filling model. C) and D) Side and top views of hNav1.7 pore-forming α-subunit with its domains and binding sites presented in ribbon representation (PDB entry: 5EK0).²⁹ Each domain is presented by the following colours: DI VSD (blue), DI PD (light blue), DII VSD (orange), DII PD (light orange), DIII VSD (yellow), DIII PD (light yellow), DIV VSD (green) and DIV PD (light green).

Table 4 The binding site of VGSC

Binding site	Ligands	Binding domains
Site 1	TTX, STX	P-loops of DI, DII, DIII and DIV
Site 2	BTX, VTD, ACT	DI-S6, DIV-S6
Site 3	α -Scorpion toxins (OD1, AaH II, Lqh II, LqhaIT), sea anemone toxins (ATX-II, anthopleurin), spider toxins (δ -atracotoxin)	Extracellular loops of DIV S3–S4
Site 4	β -Scorpion toxins (Tz1, Css4), spider toxins (ProTx-II, HwTx-IV, GpTx-1, δ -palutoxins), antibody (SVmab)	Extracellular loops of DII S1–S2 and DII S3–S4
Site 5	PbTx, CTX	DI-S6, DIV-S5
Site 6	δ -Conotoxin (δ -SVIE, TxVIA, GmVIA)	DIV-S4
Site 7	Pyrethroids, DDT	DIII-S6
LA binding site	Local anaesthetics (lidocaine), antiarrhythmics (mexiletine, flecainide), anticonvulsants (carbamazepine, lamotrigine)	DI-S6, DIII-S6, DIV-S6
SA binding site	Sulphonamides (PF-05089771, DS-1971a, GDC-0276/RG7893, GDC-0310/RG6029)	Extracellular voltage sensor of DIV-S4

Binding site 2

VGSC activators, such as the alkaloids batrachotoxin (BTX), veratridine (VTD) and aconitine (ACT), as well as several diterpenes and macrolide hoiamides bind to the open state at site 2 to stabilise the open state for activation. Binding site 2 is located in the S6 region of DI and DIV.

Binding site 3

α -Scorpion toxins, several spider toxins and anthopleurin from sea anemones bind to site 3 of VGSCs in the resting state to impair inactivation and induce a prolonged open state. Binding site 3 is found at the extracellular S3–S4 loops of DIV.

Binding site 4

Long-chain peptide toxins, such as β -scorpion toxins, several spider toxins and recombinant SVmab (rSVmab)³³ inhibit VGSCs by binding to site 4 and acting as gating modifiers that shift the activation threshold to more negative membrane potentials. Binding site 4 is located in segments S1–S2 and S3–S4 of DII.

Binding site 5

Lipophilic cyclic polyethers, such as brevetoxins (PbTx) and ciguatoxins (CTX), activate VGSCs by binding to site 5. These toxins bind to the activated state preferentially and shift the activation threshold to more negative membrane potentials. Binding site 4 is scattered in DI-S6 and DIV-S5.

Binding site 6

δ -Conotoxins impede inactivation by binding to site 6, a subsite of site 3. The location of site 6 is believed to be extracellular DIV-S4.

Binding site 7

Some insecticides, including pyrethroids and DDT, inhibit channel inactivation by binding to site 7, thereby causing persistent activation. Binding site 7 is located in DIII-S6.

Local anaesthetic (LA) binding site

Non-selective VGSC inhibitors, including local anaesthetics, class I cardiac anti-arrhythmics, anti-convulsants, and anti-depressants, bind to the LA binding site. This binding site recognises an aromatic ring and a basic moiety as a pharmacophore. Lidocaine (1), mexiletine (2), carbamazepine (3) and lacosamide (4), which are presented in Table 6, are known to bind to this site. As this site is almost conserved across VGSCs, these drugs inhibit VGSCs in a non-selective manner.³¹ The LA binding site is located in the inner cavity of the pore region, which comprises residues in DI-S6, DIII-S6 and DIV-S6. The LA binding site displays significant overlap with binding site 2.

SA binding site

Sulphonamides, which were first disclosed by Pfizer, are known to inhibit VSD4 deactivation by binding to the activated state of voltage-sensing domain IV (VSD4), thereby stabilising the inactivated state of Na_v1.7.²⁹ The profile of these molecules is discussed in the following sections.

3. *In vitro* screening technologies

Over several decades, the functional activity of VGSCs has been studied in multiple *in vitro* assay systems. Electrophysiological techniques such as the patch-clamp assay are regarded as the gold standards for the physiological and pharmacological study of ion channel function. Although the manual patch-clamp assay provides the most reliable, high temporal resolution, direct measurement of ion channel function, it is extremely low-throughput, and it requires highly skilled operators. Recently, various automated patch-clamp assay systems have been developed and launched, and they provide high-quality and high-throughput data on ion channel function.^{34–36} Fluorescence-based techniques, such as fluorescent imaging plate reader (FLIPR)- and fluorescence resonance energy transfer (FRET)-based membrane potential assays, are also widely used for high-throughput screening (HTS). Although these techniques have superior throughput in general, their

Table 5 *In vitro* screening technologies for VGSC drug discovery

Assay type	Representative example	Temporal resolution	Information content	Throughput
Binding	Radioligand binding assay	Low (h)	Low (not functional)	Mid-high
Ion flux	Radioisotope influx assay	Mid (s to min)	Mid	Mid-high
	AAS for Li^+ , Tl^+			
Fluorescence dye	FLIPR membrane potential assay	Mid (s)	Mid	High
	FRET-based membrane potential assay (e.g., VIPR)	High (ms to s)	Mid	High
Electrophysiology	Automated patch-clamp assay	High (μs to ms)	High	Mid-high
	Manual patch-clamp assay	High (μs to ms)	High	Low

AAS, atomic absorption spectroscopy; VIPR, voltage ion probe reader.

temporal resolution and biological relevancy are inferior to those of electrophysiological techniques. Ionic currents cannot be directly measured using these techniques, and their relatively high false-positive/negative rates because of compound-induced fluorescence or compound-dye interactions represent a major disadvantage.^{34,37} AstraZeneca's research group reported that the Li^+ ion flux assay was a robust and reliable assay for the HTS of VGSC targets rather than FLIPR- and FRET-based membrane potential assays.³⁸ However, in ion influx assays, the application of VTD, a VGSC activator, can produce the same drawback as fluorescence-based membrane potential assays.^{34,39} The features of *in vitro* screening technologies for VGSC drug discovery are summarised in Table 5. This review focuses on the *in vitro* activities measured by the gold standards, patch-clamp assay.

4. Perspective of state-dependent properties in electrophysiological assays

VGSCs are extremely flexible, and they can exist in three distinct voltage-dependent conformational states: resting, open and inactivated states (Fig. 2A).⁴⁰

In the resting state, the pore is closed for sodium ion conductance. When the membrane is depolarized, the voltage sensor in S4 helices moves outward to enhance pore opening, which enables sodium ion conductance within 1–2 ms. After depolarizing the membrane, VGSCs shift to an inactivated state *via* fast inactivation, in which the pore is still open but the inactivation gate located between DIII and DIV prevents ion conductance. Then, the channel moves to a slow inactivated state in response to prolonged depolarization or rapid repetitive stimulations. Fast inactivation occurs on a millisecond time scale, whereas slow inactivation occurs on the timescale of seconds to minutes. The activation of voltage sensor S4 across DI–DIII contributes to channel activation, whereas the activation of DIV–S4 leads to the movement of the IFM motif in the inactivation gate, resulting in channel inactivation. Finally, membrane hyperpolarisation leads to the channel resting state.

Thus, inhibition of VGSC can be achieved in two distinguished manners: 1) direct pore-blocking mechanism and 2) stabilisation of a certain state, which inhibits shifting to the next state. Many VGSC inhibitors including medicinal

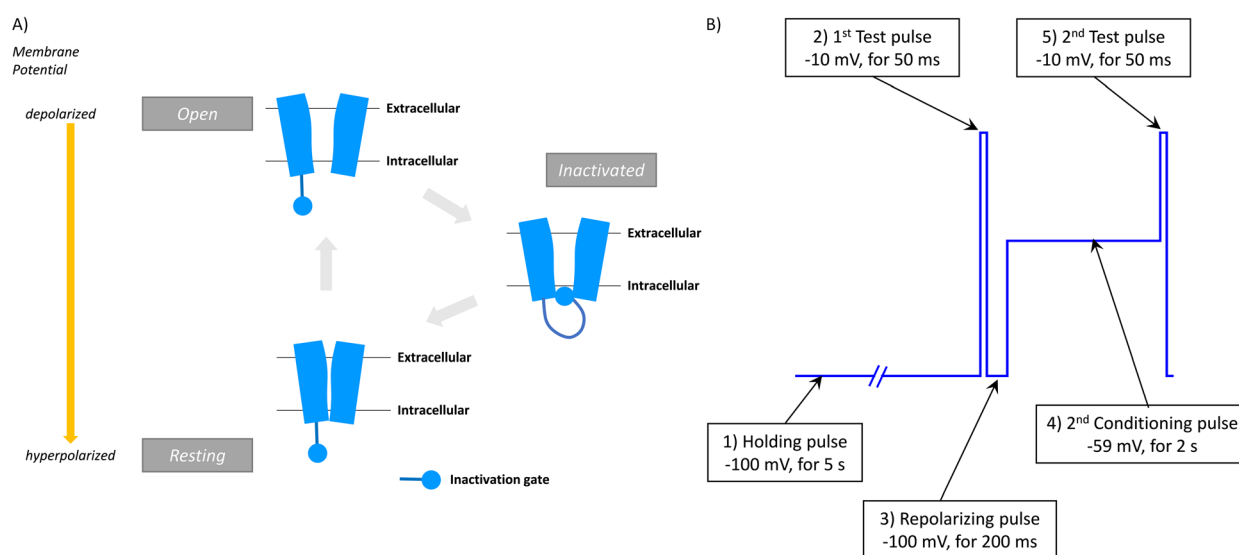


Fig. 2 Voltage-dependent conformational changes of VGSCs. A) Three distinct voltage-dependent conformational states: resting, open and inactivated states. B) An example of voltage protocol for an automated patch-clamp assay that permits evaluation of both resting (V_{rest}) and inactivated ($V_{1/2}$) states of $\text{hNa}_v1.7$.³⁶

drugs preferentially bind and interact with specific conformations or states. This state-dependent inhibition is also associated with the accumulation of inhibition, also called use-dependent inhibition or frequency-dependent inhibition.⁴¹ State-dependent inhibition is considered to impart functional selectivity to drug effects. For example, if a drug preferentially binds to a specific channel conformation and the conformation is dominant in a specific disease state or in the target organ or tissue for drug treatment, state-dependent inhibition can confer great benefits regarding both efficacy and safety. In fact, the clinical utility of state-dependent and/or use-dependent VGSC inhibitors has been demonstrated in cardiac arrhythmia,⁴² epilepsy⁴³ and chronic pain.^{44,45} Therefore, it is extremely important to evaluate real channel function and drug effects according to individual conformational states. The patch-clamp assay is an unparalleled technique that fulfils the aforementioned demands based on its comprehensive and flexible analyses. Recently, efficient and effective pulse protocols for automated patch-clamp systems that permit the evaluation of both resting and inactivated channel states have been reported.^{22,36,46} In primary screening at our laboratory, the effects of compounds in both resting (V_{rest}) and inactivated (half-maximal voltage [$V_{1/2}$]) states were determined with one protocol using an automated patch-clamp system (Fig. 2B).^{47,48}

In chronic pain states, especially NP, ectopic discharges from primary sensory neurons represent a characteristic phenomenon. This pathological phenomenon is considered to result from the membrane potential oscillation mechanism rather than the traditional Hodgkin–Huxley model, which features a repetitive firing process.⁴⁴ In rat DRG neurons, membrane potential oscillations exhibit voltage-sensitive properties. Namely, the prevalence of oscillations and consequent ectopic discharges is higher in depolarised states than in the resting state, and furthermore, those changes are enhanced after sciatic nerve injury.⁴⁹ It is apparent that TTX-sensitive VGSCs contribute to the generation of membrane potential oscillations in DRG neurons. Thus, it might be useful to evaluate the effects of drugs on VGSCs under more depolarised states (*i.e.*, pathological states) as well as physiological states. In fact, we found a series of compounds that selectively inhibit $Na_v1.7$ currents in a more depolarised state (at the holding potential of -30 mV) but not in the resting or inactivated state, resulting in potent analgesic effects with a wide safety margin in NP model mice.⁴⁷

5. Conventional VGSC inhibitors

Non-selective VGSC inhibitors have been studied for decades, and their utility has been proven in clinical settings.^{42–44,50} Their common characteristics are weak VGSC inhibitory activity with modest subtype selectivity. Their inhibitory activity is usually in the micromolar range.

Lidocaine (**1**) is a classical non-selective VGSC inhibitor that has been used as local anaesthesia, whereas mexiletine (**2**) can be used as an oral analgesic agent. Carbamazepine (**3**)

treats CNS disorders, including epilepsy. As presented in Table 6, these compounds weakly inhibit VGSC without high subtype selectivity.^{36,46} Classical non-selective VGSC inhibitors are useful; in particular, topical lidocaine (lidocaine patch) can significantly relieve various pain disorders by restricting systemic exposure.⁵² Thus, if a certain safety window can be obtained according to the formulation or route of administration, non-selective VGSC inhibitors could be launched for the treatment of pain disorders.

Lacosamide (**4**) is a broad VGSC inhibitor that was efficacious in patients with diabetes and NP in phase 2 clinical trials without an approval for NP indications.⁵³ It was reported that lacosamide attenuated cold (from 10 mg kg^{-1} , IP), warm (from 3 mg kg^{-1} , IP) and mechanical allodynia (30 mg kg^{-1} , IP) in rats with streptozotocin (STZ)-induced diabetes.⁵⁴

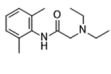
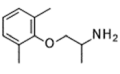
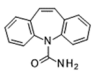
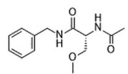
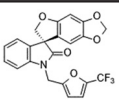
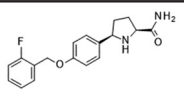
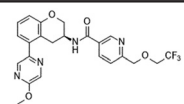
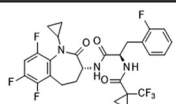
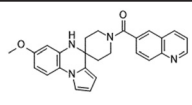
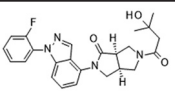
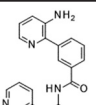
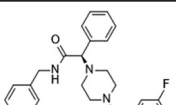
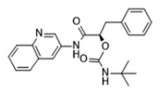
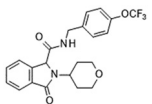
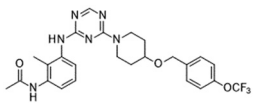
Funapide (**5**: XEN402/XPF-002/TV-45070/FX301) was developed by Xenon and Teva for the treatment of several pain disorders as a topical formulation, and it is under development as FX-301, an extended-release, locally-delivered, thermosensitive hydrogel formulation, by Flexion Therapeutics. Funapide is a potent state-dependent VGSC inhibitor with IC_{50} values of 601 , 84 , 173 and 54 nM for $Na_v1.2$, $Na_v1.5$, $Na_v1.6$ and $Na_v1.7$, respectively.⁵⁵

Biogen Inc. is developing vixotrigine (**6**: raxatrigine/BIB074/CNV1014802/GSK1014802), which both inhibits multiple subtypes of VGSCs and exhibits MAO-B inhibitory activity.^{46,56–58} Vixotrigine was reported to inhibit multiple VGSCs in a state- and use-dependent manner. The consecutive administration of vixotrigine significantly reversed mechanical allodynia in a chronic constriction injury (CCI) model of NP at a dose of 0.5 or 5 mg kg^{-1} , p.o. BID (twice daily). Free plasma concentrations on day 8 after administration for 0.5 h per day were 6.0 and 74 nM at doses of 0.5 and 5 mg kg^{-1} , respectively. A single oral dose of vixotrigine was also efficacious in a Complete Freund's Adjuvant (CFA) rodent model with an ED_{50} of 0.91 mg kg^{-1} . The free plasma concentration reached 25 nM at a dose of 1 mg kg^{-1} , p.o.⁵⁷ Thus, the *in vivo* efficacious free plasma concentration was more than 100-fold smaller than that reported for each human VGSC *in vitro* because it was noted that rodent $Na_v1.7$ and $Na_v1.8$ activities were comparable to those of humans. Vixotrigine is under development for the potential treatment of NP and trigeminal neuralgia.⁵⁹

AZD3161 (**7**) was developed by AstraZeneca, and it exhibited high $hNa_v1.7$ inhibitory activity with good selectivity over $hNa_v1.5$. AZD3161 displayed antinociceptive effects dose-dependently in the rat phase 1 formalin test. A statistically significant antinociceptive effect was detected at 23 mg kg^{-1} , and the plasma concentration at this dose was 5 μ M.⁶⁰

Merck reported the discovery of benzazepinone **8** and pyrrolo-benzo-1,4-diazine **9**.^{61,62} Both compounds displayed comparable $hNa_v1.7$ inhibitory activity, whereas **9** exhibited improved selectivity over $hNa_v1.5$. Compound **8** inhibited $hNa_v1.7$ with K_i values of 0.44 μ M in the inactivated state and 24 μ M in the resting state. **8** induced dose-dependent reversal in a rat spinal nerve ligation (SNL) model of NP with

Table 6 Conventional VGSC inhibitors with their *in vitro* profiles, free plasma concentrations and Na_v1.7 coverage^a

			
Lidocaine (1) ³⁶	Mexiletine (2) ³⁶	Carbamazepine (3) ⁴⁶	Lacosamide (4) ⁵¹
hNa _v 1.1 IC ₅₀	—	>100 μM ^{b,d}	—
hNa _v 1.5 IC ₅₀	50 μM ^{b,c}	46.8 μM ^{b,d}	—
hNa _v 1.7 IC ₅₀	16 μM ^{b,c}	91.3 μM ^{b,d}	182 μM ^{c,e}
			
Funapide (5) ⁵⁵	Vixotrigine (6)	AZD3161 (7) ⁶⁰	8: Merck ⁶²
hNa _v 1.1 IC ₅₀	—	—	—
hNa _v 1.5 IC ₅₀	0.084 μM	12.6 μM ^b	2.38 μM (K _i) ^{c,e}
hNa _v 1.7 IC ₅₀	0.054 μM	0.079 μM ^{b,g}	0.44 μM (K _i) ^{c,e}
Free plasma concentration	—	5 μM@23 mg kg ^{-1h} (rat formalin)	0.53 μM@1 mg kg ^{-1h,i} (rat PK)
			
9: Merck ⁶¹	10: AbbVie ⁶³	11: Amgen ⁶⁴	12: Amgen ⁶⁵
hNa _v 1.1 IC ₅₀	—	—	—
hNa _v 1.5 IC ₅₀	17.9 μM ^{e,j}	3.9 μM ^{b,c}	0.95 μM ^{b,c}
hNa _v 1.7 IC ₅₀	0.69 μM ^{e,j}	0.15 μM ^{b,k}	0.37 μM ^{b,k}
Rodent Na _v 1.7 IC ₅₀	—	0.049 μM (rat) ^{b,k}	0.46 μM (mouse) ^{b,k}
Rodent PPB ^f	99% (rat)	82.2% (rat)	96.3% (mouse)
Free plasma concentration	0.72 μM@ <i>in vivo</i> EC ₅₀ (rat SNL)	5.7 μM@ <i>in vivo</i> EC ₅₀ (acute, rat MIA) ^h 1.8 μM@ <i>in vivo</i> EC ₅₀ (subchronic, rat MIA) ^h	61, 280 nM@30, 100 mg kg ⁻¹ (rat formalin)
Na _v 1.7 coverage in plasma@efficacious dosage ^a	—	>5.7-Fold@100 mg kg ⁻¹ (rat formalin)	1.8-Fold@300 mg kg ⁻¹ (mouse histamine)
			
13: Daiichi Sankyo ⁴⁷	14: AstraZeneca ⁶⁹	15: Amgen	
hNa _v 1.1 IC ₅₀	>100 μM ^{b,c}	—	—
hNa _v 1.5 IC ₅₀	>100 μM ^{b,c}	>30 μM ^{b,m}	1.1 μM ^{e,n,70}
hNa _v 1.7 IC ₅₀	5.2 μM ^{b,i}	0.41 μM ^{b,g}	0.17 μM ^{e,n,70}
Rodent Na _v 1.7 IC ₅₀	11.8 μM (mouse) ^{b,i}	1.6 μM (rat) ^{b,g}	0.39 μM (rat) ^{e,n,71}
Rodent PPB ^f	98.96% (mouse)	86.8% (rat)	97.3% (rat) ⁷¹
Free plasma concentration	2.7 nM@30 mg kg ⁻¹ⁱ (mouse PK)	400 nM@43 mg kg ⁻¹ (rat formalin)	14, 38 nM@3, 10 mg kg ⁻¹ (rat formalin) ⁷⁰ 67 nM@10 mg kg ⁻¹ (rat CFA) ⁷¹
Na _v 1.7 coverage in plasma@efficacious dosage ^a	0.000025-Fold@3.3 mg kg ⁻¹ⁱ (PSNL mouse)	0.25-Fold@43 mg kg ⁻¹ (rat formalin)	0.035-, 0.097-fold@3, 10 mg kg ⁻¹⁷⁰ (rat formalin) 0.17-Fold@10 mg kg ⁻¹⁷¹ (rat CFA)

^a Na_v1.7 coverage = free plasma concentration/*in vitro* Na_v1.7 IC₅₀. ^b Value in the automated patch-clamp assay. ^c Value in an inactivated state. ^d Value at V_{hold} = -60 mV. ^e Value in the manual patch-clamp assay. ^f Plasma protein binding. ^g Value at V_{hold} = -65 mV. ^h Plasma concentration. ⁱ Calculated from C_{max} of the PK study. ^j Value at V_{hold} = -120 mV. ^k Value in a slow-inactivated state induced by prolonged depolarisation to -20 mV. ^l Value at V_{hold} = -30 mV. ^m Value at V_{hold} = -90 mV. ⁿ Value when approximately 20% of the channels were inactivated.

an ED₅₀ of 15 mg kg⁻¹. As C_{max} was reported as 0.53 μM at a dose of 1 mg kg⁻¹, p.o. in the PK study, C_{max} is expected to

approach 8 μM at ED₅₀. No impaired motor coordination was observed at 100 mg kg⁻¹.⁶² Compound 9 displayed better

Na_v1.5 selectivity than **8**. Compound **9** inhibited hNa_v1.7 with an IC₅₀ of 0.69 μM, and it was efficacious in a rat CFA-induced inflammatory pain model at 100 mg kg⁻¹ with statistical significance. Compound **9** was also efficacious in a rat SNL NP model with EC₅₀ = 72 μM, which was comparable to that for Na_v1.7 (IC₅₀ = 33 μM) in the presence of 100% rat serum. Low exposure in the brain (brain K_p brain at 6 h = 0.2) was noted.⁶¹

AbbVie reported a selective Na_v1.7 inhibitor **10** that inhibited hNa_v1.7 with IC₅₀ = 0.34 μM and 100-fold selectivity over hNa_v1.5. Compound **10** was efficacious at 10 mg kg⁻¹ in a monosodium iodoacetate (MIA)-induced osteoarthritis (OA) rat model (EC₅₀ = 5.7 μM). The efficacy was enhanced by subchronic dosing twice a day for 7 days, which enhanced the efficacy at a dose of 0.3 mg kg⁻¹ by achieving the same plasma levels as higher doses (EC₅₀ = 1.8 μM).⁶³

Amgen reported the discovery of compound **11**. In their assay protocol, hNa_v1.7 activity was measured at a slow-inactivated state induced by prolonged depolarisation to -20 mV, whereas the hNa_v1.5 assay was conducted at holding partial channel inactivation. As compound **11** failed to exhibit significant efficacy in a rat formalin pain model at 100 mg kg⁻¹ with Na_v1.7 coverage of 5.7-fold, they concluded that binding to a slow-inactivated state of Na_v1.7 may not significantly alter *in vivo* target coverage requirements.⁶⁴

In the same year, Amgen disclosed the identification of the early lead compound piperazine **12**, which was evaluated under the same *in vitro* assay protocol. Although **12** displayed comparable *in vitro* inhibitory activities as **11**, it was efficacious in a mouse histamine-induced pruritus model with 1.8-fold target coverage. A subsequent SAR study led to the identification of the compounds with better Na_v1.5 selectivity, although their *in vivo* efficacy was not evaluated.⁶⁵ In this review article, the target coverage or Na_v1.7 coverage was defined using the following formula for clear discussion on the extent of target coverage required to achieve certain *in vivo* efficacy: Na_v1.7 coverage (fold) = free plasma concentration/*in vitro* Na_v1.7 IC₅₀.

Our group disclosed compound **13**⁴⁷ derivatised from the report by Merck.^{62,66–68} Compound **13** inhibited Na_v1.7 in a state-dependent manner. Although compound **13** was inactive at V_{1/2} (V_{hold} = -59 mV), it inhibited hNa_v1.7 at V_{hold} = -30 mV (IC₅₀ = 5.2 μM). Compound **13** was effective against thermal hyperalgesia in Seltzer (partial sciatic nerve ligation [PSNL]) model mice (ED₅₀ = 3.3 mg kg⁻¹). Notably, compound **13** displayed a good safety margin against CNS adverse effects with a suitable value of K_p in the brain (0.69). The target coverage of compound **13** was 0.00025-fold based on the reported PK parameters and plasma binding ability. Compound **13** exhibited modest selectivity because it did not affect other channels, receptors and transporters at 10 μM given its modest Na_v1.7 IC₅₀ values (5.2 μM for humans, 11.8 μM for mice).⁴⁷

AstraZeneca disclosed an oxoisindoline derivative **14**. As compound **14** exhibited hNa_v1.7 (IC₅₀ = 0.41 μM at V_{hold} = -65 mV and hNa_v1.7 IC₅₀ = 3.8 μM at V_{hold} = -90 mV), it was

considered a state-dependent Na_v1.7 inhibitor. Compound **14** was inactive at several other channels but efficacious in the phase 1 reaction of a rat formalin model at 43 mg kg⁻¹. The free plasma concentration of **14** was 400 nM at the end of the formalin assay, which corresponds to 0.25-fold of the rat Na_v1.7 IC₅₀. A site-directed mutagenesis study suggested that oxoisindoline derivatives bound to the local anaesthetic site of Na_v1.7.⁶⁹

Triazine **15** is a Na_v1.7 inhibitor with modest Na_v1.5 selectivity that was disclosed by Amgen. Compound **15** is a state-dependent inhibitor with an IC₅₀ of 170 nM at hNa_v1.7 when 20% of the channels were inactivated and 3.6 μM in the resting state. Compound **15** was efficacious in phase 2 in a rat formalin model from 3 mg kg⁻¹ with statistical significance, and the maximum effect at 30 mg kg⁻¹ was equivalent to that produced by morphine. However, **15** significantly reduced movement from 20 mg kg⁻¹. The Na_v1.7 coverage was 0.035-fold at 3 mg kg⁻¹ and 0.097-fold at 10 mg kg⁻¹.^{70,71} **15** also reversed thermal hyperalgesia in a CFA model at 10 mg kg⁻¹. The plasma concentration at a dose of 10 mg kg⁻¹ reached 2.48 μM, and its target coverage was 0.17-fold. Brain exposure (0.81 μM) was observed for **15** at 10 mg kg⁻¹. **15** was suggested not to affect the spontaneous activity or evoked responses of Aδ-fibres, but C-fibre nociceptors were indicated to regulate spontaneous discharge and cause analgesia based on the electrophysiological results of rat single nociceptive fibres in the CFA assay.⁷¹

Although some Na_v1.7 inhibitors such as **11** failed to demonstrate potent *in vivo* efficacy, these conventional inhibitors tend to exhibit higher *in vivo* efficacy than predicted by PK and *in vitro* VGSC potency. Vixotrigine (**6**) displayed robust *in vivo* efficacy with a lower free plasma concentration (25 nM) than needed for *in vitro* VGSC activity (by over 100-fold at the ED₅₀ dose), and the Na_v1.7 coverage of compound **13** was extremely small at the ED₅₀ dose. Compounds **14** and **15** were effective in a rat formalin assay with less than 1-fold Na_v1.7 coverage.

One of the causes of poor PK/PD correlations is weak *in vitro* Na_v1.7 potency. As the mode of action (MOA) of vixotrigine covers multiple targets, it is possible that this compound demonstrated potent efficacy in rodents *via* the synergic effect of multiple MOAs. As Na_v1.6 is also involved in pain signalling pathways other than Na_v1.3, Na_v1.7, Na_v1.8 and Na_v1.9 signalling, the contribution of Na_v1.6 inhibition may not be ignored.^{40,72} However, the potent *in vivo* efficacy of compound **13** can be hardly explained because it exhibited modest selectivity over other targets.⁴⁷ As one possible reason is the contribution of the active metabolites, such studies are expected to resolve this issue to some extent.

Although the MOAs of potent *in vivo* efficacy remain controversial, some conventional VGSC inhibitors are efficacious in both animal models and patients. This indicates the possibility that these inhibitors could be future analgesics if a sufficient safety window is obtained in both preclinical animals and humans.

6. Sulphonamides

In 2010, Pfizer disclosed a highly potent selective $\text{Na}_V1.7$ inhibitor in their patent,²⁷ followed by the initiation of clinical trials of PF-05089771 (**16**).^{73,74} As presented in Table 7, PF-05089771 inhibited $\text{hNa}_V1.7$ with an IC_{50} of 15 nM and excellent subtype selectivity over $\text{hNa}_V1.1$ and $\text{hNa}_V1.5$. A mutational study revealed that PF-05089771 interacted with VSD4 because the compound was not substantially affected by mutation of either the TTX or local anaesthetic binding sites, whereas its inhibitory activity was greatly affected by the $\text{hNa}_V1.7$ M1,2,3 mutation.⁷⁵ PF-05089771 inhibited $\text{hNa}_V1.7$ in a state-dependent manner, and its IC_{50} for $\text{hNa}_V1.7$ at the resting state exceeded 10 μM .⁷⁵ PF-05089771 inhibited the rat orthologue with 10-fold lower potency than it inhibited the human orthologue, and the lack of potent activity against the rat orthologue was explained by the sequence divergence at VSD4, the binding site for sulphonamides.^{75,76} This opened a new era for the development of sulphonamide derivatives as potent selective $\text{Na}_V1.7$ inhibitors, and many pharmaceutical and biotech firms disclosed their analogues. Some of them utilised PF-05089771 as a tool compound and reported the preclinical efficacy of their compounds. For example, Xenon and Genentech reported an evaluation of PF-05089771. In their article, they mentioned that 82-fold target coverage was required for robust efficacy in a transgenic mouse model expressing human $\text{Na}_V1.7$ with an IEM mutation (I848T, IEM transgenic mouse).^{77,78} The clinical efficacy of PF-05089771 is discussed in the following section.

The Xenon/Genentech group disclosed compound **17**. They successfully obtained compound **17** with high rat $\text{Na}_V1.7$ activity, which enabled *in vivo* evaluation in this animal. Because compound **17** failed to display sufficient plasma accumulation in rats following oral administration, *in vivo* assessments were conducted *via* IP administration. Compound **17** significantly reduced the pain response in the phase 2 formalin assay at 100 mg kg^{-1} IP. Compound **17** was also effective against acute pain evoked by aconitine as a pain stimulus at 100 mg kg^{-1} IP. The required $\text{Na}_V1.7$ coverage was 10-fold for robust efficacy in both assays. Compound **17** was also efficacious against CFA-induced cold allodynia in mice.⁷⁹

Lupin reported an indane derivative **18** with excellent subtype selectivity. Compound **18** induced the state-dependent blockade of $\text{hNa}_V1.7$ and led to slow inactivation of $\text{hNa}_V1.7$ with an IC_{50} of 33 nM, whereas **18** induced rapid inactivation with an IC_{50} of 99.7 nM. Compound **18** displayed high efficacy against veratridine-induced nociceptive behaviours from 10 mg kg^{-1} , phase 2 formalin-induced nociceptive behaviour from 3 mg kg^{-1} and CCI-induced allodynia at 100 mg kg^{-1} with statistical significance in mice. The unbound plasma concentration of **18** at the end of the formalin study at 3 mg kg^{-1} was 0.343 μM , which is 10-fold higher than the $\text{mNa}_V1.7$ IC_{50} .⁸⁰

Our group disclosed the discovery of DS-1971 (**19**), a potent selective $\text{Na}_V1.7$ inhibitor, which inhibited $\text{hNa}_V1.7$ with IC_{50} = 22.8 nM and high subtype selectivity. DS-1971 displayed

potent analgesic efficacy in PSNL mice. DS-1971 displayed efficacy against mechanical hypersensitivity from 1 mg kg^{-1} , and it exhibited potent efficacy against thermal hyperalgesia from 0.3 mg kg^{-1} with statistical significance. Hence, DS-1971 displayed potent efficacy at less than 1-fold target coverage. The unique kinetics of DS-1971 was reported. DS-1971 exhibited a slower onset of inhibition than mexiletine, whereas the dissociation velocity of DS-1971a was slower than that of mexiletine. We concluded that this unique kinetics contributed to the potent efficacy of DS-1971.⁴⁸

Amgen reported AM-0466 (**20**) with an IC_{50} of 21 nM for $\text{hNa}_V1.7$. AM-0466 reduced scratching bouts in a histamine-induced pruritus mouse model in a dose-dependent manner, and a statistically significant reduction of itching behaviour was achieved at 30 mg kg^{-1} . The unbound plasma concentration of **20** was 0.49 μM at a dose of 30 mg kg^{-1} , which resulted in target coverage of 16-fold *versus* the $\text{mNa}_V1.7$ IC_{50} . AM-0466 was also efficacious in a mouse capsaicin-induced nociception pain model at 100 and 300 mg kg^{-1} , which generated unbound plasma concentrations of 1.3 and 1.7 μM , respectively, resulting in target coverage values of 43- and 57-fold, respectively, over the $\text{mNa}_V1.7$ IC_{50} .⁸¹

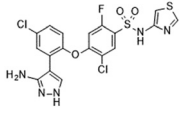
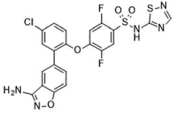
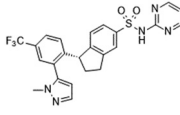
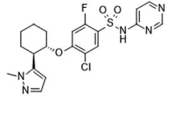
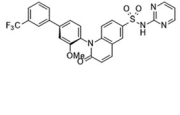
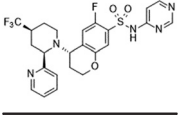
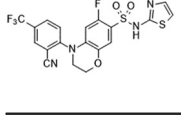
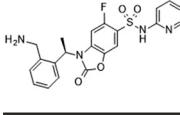
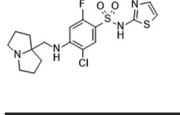
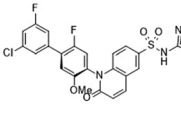
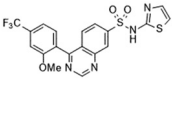
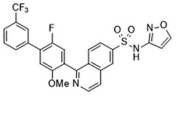
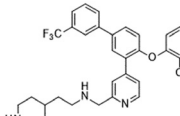
Genentech reported the identification of GNE-616 (**21**). This compound inhibited $\text{hNa}_V1.7$ at K_d = 0.38 nM with excellent subtype selectivity. PK/PD analysis revealed that **21** reduced nociceptive events with EC_{50} = 740 nM (unbound $\text{EC}_{50,u}$ = 9.6 nM) in an IEM aconitine mouse model, which corresponded to 25-fold $\text{hNa}_V1.7$ coverage.⁸²

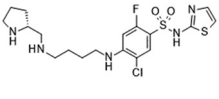
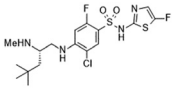
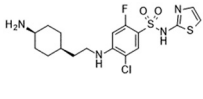
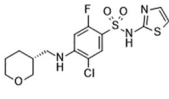
Amgen disclosed a tool compound **22** with potent rat $\text{Na}_V1.7$ inhibitory activity, although this compound lost high selectivity against $\text{hNa}_V1.5$. Compound **22** was efficacious in phase 2 of a formalin rat model at 30 and 100 mg kg^{-1} . These doses produced plasma coverage of 1.3 and 3.6-fold over the rat $\text{Na}_V1.7$ IC_{50} , respectively. *In vivo* assessments were also conducted in mice, and higher target coverage (more than 6-fold) was needed for high *in vivo* efficacy in the formalin test in mice with histamine-induced pruritus.⁸³

The discovery of benzoxazolinone **23** was reported by Merck. Compound **23** was effective in phase 2 in a mouse formalin model from 20 mg kg^{-1} , and the *in vivo* IC_{50} was calculated as 7.4 μM (unbound $\text{IC}_{50,u}$ = 1.1 μM), which is 100-fold higher than the *in vitro* potency in mice.⁸⁴ The Merck group also reported the identification of compound **24**, which displayed statistically significant efficacy in phase 2 in the mouse formalin model from 3 mg kg^{-1} . The unbound plasma concentration at *in vivo* $\text{IC}_{50,u}$ was 170 nM, which was 11-fold higher than the $\text{mNa}_V1.7$ IC_{50} . Compound **24** is also efficacious in the histamine-induced itch assay in mice. Compound **24** induced a dose-dependent blockade of scratching events, and complete blockade was achieved at 30 mg kg^{-1} .⁸⁵ Later, the Xenon/Genentech group reported an evaluation of **24** and disclosed that 28-fold target coverage was needed to elicit significant efficacy in IEM transgenic mice.⁷⁷

AMG8379 (**25**) was reported to block mechanically induced action potential firing in C-fibres, whereas the less active enantiomer AMG8380 had no such effects. AMG8379 was

Table 7 Sulphonamide derivatives with their *in vitro* profiles and target coverage^a

				
PF-05089771 (16)	Xenon/Genentech (17) ⁷⁹	18: Lupin ⁸⁰	DS-1971 (19) ⁴⁸	AM-0466 (20) ⁸¹
hNav _v 1.1 IC ₅₀	677 nM ^{c,d,73}	3080 nM ^{d,e}	>10 000 nM ^{d,e}	>42 500 nM ^{c,h}
hNav _v 1.5 IC ₅₀	>10 000 nM ^{c,d,73}	1380 nM ^{d,e}	>10 000 nM ^{d,e}	>42 500 nM ^{c,h}
hNav _v 1.7 IC ₅₀	15 nM ^{c,d,73} , 3.9 nM ^{e,f,73}	0.4 nM ^{d,e}	33 nM ^{d,e}	21 nM ^{c,h}
Mouse Nav _v 1.7 IC ₅₀	8 nM ^{c,d,75}	0.2 nM ^{d,e} (rat: 26 nM ^{d,e})	33 nM ^{d,e}	30 nM ^{c,h}
Mouse PPB ^b	98.7%, ⁷⁷ 99.9% ⁹⁰	(rat: 98.9%)	92.9%	—
Nav _v 1.7 coverage in plasma@efficacious dosage ^a	82-Fold@ <i>in vivo</i> IC ₅₀ (IEM mouse) ⁷⁷	10-Fold@100 mg kg ⁻¹ (IP) (rat formalin, rat aconitine)	10-Fold@3 mg kg ⁻¹ 39-Fold@10 mg kg ^{-1g} (mouse formalin)	0.058, 0.26-fold@1, 3 mg kg ^{-1g} (PSNL mouse) 16-Fold@30 mg kg ⁻¹ (mouse histamine) 43-, 57-fold@100, 300 mg kg ⁻¹ (mouse capsaicin)
				
GNE-616 (21) ⁸²	22: Amgen ⁸³	23: Merck ⁸⁴	24: Merck	
hNav _v 1.1 IC ₅₀	>1000 nM (K _d) ^{e,f}	—	—	—
hNav _v 1.5 IC ₅₀	>1000 nM (K _d) ^{e,f}	330 nM ^{e,i}	33 000 nM ^{c,d}	>30 000 nM ^{c,d,85}
hNav _v 1.7 IC ₅₀	0.38 nM (K _d) ^{e,f}	140 nM ^{e,i}	39 nM ^{c,d}	8 nM ^{c,d,85} , 3.1 nM ^{e,f,77} 2.4 nM ^{e,j,93}
Mouse Nav _v 1.7 IC ₅₀	—	60 nM ^{e,i} (rat: 70 nM ^{e,i})	11 nM ^{c,d}	15 nM ^{c,d,85} , 3.9 nM ^{e,j,93,95} 1.8 nM ^{e,j,k,95}
Mouse PPB ^b	98.70%	99.4% (rat: 98.5%)	85.5%	59%, ⁸⁵ 78%, ⁷⁷ 76% ^{93,95}
Nav _v 1.7 coverage in plasma@efficacious dosage ^a	25-Fold@ <i>in vivo</i> EC ₅₀ (IEM mouse)	1.3-Fold, 3.6-fold@30, 100 mg kg ⁻¹ (rat formalin) 10-Fold, 16-fold@60, 100 mg kg ⁻¹ (mouse formalin) 6-Fold, 10-fold, 11-fold@30, 60, 100 mg kg ⁻¹ (mouse histamine)	100-Fold@ <i>in vivo</i> EC ₅₀ (mouse formalin)	11-Fold@ <i>in vivo</i> IC ₅₀ ⁸⁵ (mouse formalin) 28-Fold@ <i>in vivo</i> IC ₅₀ ⁷⁷ (IEM mouse) 326-Fold@60 mg kg ⁻¹ ⁹² 21-Fold@60 mg kg ⁻¹ , ⁹² 87-Fold@30 mg kg ⁻¹ ⁹⁴ 189-Fold@30 mg kg ⁻¹ , ⁹⁴ (mouse formalin)
				
AMG8379 (25) ⁸⁶	26: Amgen ⁸⁸	27: Amgen ⁸⁸	28: Pfizer ⁸⁹	
hNav _v 1.1 IC ₅₀	>14 000 nM ^{c,n}	7300 nM ^{e,o}	17 000 nM ^c	314 nM ^{c,d}
hNav _v 1.5 IC ₅₀	>14 000 nM ^{c,n}	16 000 nM ^{e,o}	12 000 nM ^c	2592 nM ^{c,d}
hNav _v 1.7 IC ₅₀	8.5 nM ^{c,h} , 3.2 nM ^{c,n}	140 nM ^{e,o}	17 nM ^c	0.01 nM ^{c,d}
Mouse Nav _v 1.7 IC ₅₀	18.6 nM ^{c,h} , 16.8 nM ^{c,n}	180 nM ^{c,o}	36 nM ^c	<0.1 nM ^{c,d}
Mouse PPB ^b	99.83%	96.45%	98.84%	99.719%
Nav _v 1.7 coverage in plasma@efficacious dosage ^a	5.3-Fold@30 mg kg ⁻¹ (mouse histamine) 23-Fold@100 mg kg ⁻¹ (UVB-induced thermal hyperalgesia in mice) 21-Fold@100 mg kg ⁻¹ (mouse capsaicin)	28-Fold@60 mg kg ⁻¹ (mouse histamine)	45-Fold@300 mg kg ⁻¹ (mouse histamine)	>62.5-Fold@5.4 mg kg ⁻¹ (i.v.) (mouse formalin)

	 29: Merck ⁹⁰	 30: Merck ⁹¹	 31: Bristol-Myers Squibb ⁹²	 32: Bristol-Myers Squibb ⁹³
hNav _v 1.1 IC ₅₀	9000 nM ^{c,i}	—	—	—
hNav _v 1.5 IC ₅₀	>33 000 nM ^{c,i}	>34 000 nM ^{e,p}	1900 nM ^{c,o}	6400 nM ^{c,o}
hNav _v 1.7 IC ₅₀	66 nM ^{e,i}	87 nM ^{e,p}	4.0 nM ^{e,j}	78 nM ^{e,f}
Mouse Nav _v 1.7 IC ₅₀	295 nM (rhesus) ^{e,i}	8800 nM ^{e,p}	7.5 nM ^{e,j}	54 nM ^{e,f} , 34 nM ^g
Mouse PPB ^b	92.63% (rhesus)	94%, 98% (rhesus)	92%	97.7%, 90% ^r
Nav _v 1.7 coverage in plasma@efficacious dosage ^a	12-Fold, 42-fold@12.06, 24.12 mg kg ⁻¹ (i.v., rhesus OB) 1.9-Fold@20 mg kg ⁻¹ (s.c., thermal stimulus in rhesus)	0.04-Fold@ <i>in vivo</i> EC ₉₀ (mouse formalin) 4.8-Fold@19.2 mg kg ⁻¹ (rhesus OB)	>43-Fold@100 mg kg ⁻¹ >0.77-Fold@100 mg kg ^{-1l} (mouse formalin)	14-Fold@100 mg kg ⁻¹ (mouse CCI) 0.5-Fold, 1-fold@30, 60 mg kg ⁻¹ (mouse CFA) 3-Fold@30 mg kg ⁻¹ 1-Fold@30 mg kg ^{-1m} (mouse formalin)

^a Nav_v1.7 coverage = free plasma concentration/*in vitro* Nav_v1.7 IC₅₀. ^b Plasma protein binding. ^c Value in the automated patch-clamp assay. ^d Value in an inactivated state. ^e Value in the manual patch-clamp assay. ^f Value at V_{hold} = -60 mV. ^g Calculated from C_{max} of the PK study. ^h Value at a voltage yielding 20–50% channel inactivation. ⁱ Value at a voltage yielding approximately 20% channel inactivation. ^j Value at V_{hold} = -70 mV. ^k IC₅₀ of mouse DRG Nav_v1.7. ^l The target coverage in the DRG given the plasma protein binding as an estimate of tissue binding. ^m Nav_v1.7 coverage in the DRG: free DRG concentration/*in vitro* IC₅₀ of mouse DRG Nav_v1.7. ⁿ 5-Hz use-dependent voltage protocol. ^o Value at V_{hold} = -50 mV. ^p Value under a hyperpolarised assay protocol. ^q IC₅₀ of TTX-S currents in the mouse DRG. ^r Value of the mouse DRG.

examined in a variety of mouse models. The compound displayed robust efficacy against histamine-induced scratching from 30 mg kg⁻¹, at which the target coverage was 5.3-fold higher than the mNav_v1.7 IC₅₀. In UVB-induced thermal hyperalgesia and acute capsaicin-induced nociception, AMG8379 exhibited significant efficacy at 100 mg kg⁻¹, and the target coverage values were 23- and 21-fold, respectively.⁸⁶

Compounds **26** and **27** are selective Nav_v1.7 inhibitors reported by Amgen. Both compounds suppressed scratching behaviour in a histamine-induced scratching mouse model at 60 and 300 mg kg⁻¹, which corresponded to free plasma concentrations of 5.1 and 1.59 μM, respectively, with target coverage values of 28- and 45-fold higher than the mNav_v1.7 IC₅₀, respectively. As the brain K_p of compound **26** was 0.008 in mice, the authors concluded that the efficacy was the result of Nav_v1.7 inhibition in the PNS.^{87,88}

Pfizer disclosed the tool compound **28**. This compound was not efficacious in a mouse formalin model with i.v. infusion even though its free plasma concentration exceeded the mNav_v1.7 IC₅₀ by more than 62.5-fold.⁸⁹

Merck reported *in vivo* pharmacology results in rhesus monkeys. The evaluation of *in vivo* assays used two models: odour-induced activation of the olfactory bulb (OB) and noxious heat-evoked pain behaviours. Compound **29** was evaluated for its effects on membrane potential when approximately 20% of the channels were inactivated. Compound **29** inhibited rhesus Nav_v1.7 with an IC₅₀ of 295 nM, versus 926 nM for PF-05089771 (**16**) in their assay protocol. Compound **29** significantly inhibited odour-induced olfaction of OB in rhesus monkeys at two doses (12.06 and 24.12 mg kg⁻¹, i.v.), resulting in target coverage values of 12- and 42-fold, respectively. In this assay, **16** at 9.5 mg kg⁻¹ (i.v.) was not efficacious with target coverage of 0.12-

fold based on the reported value (rhesus Nav_v1.7 IC₅₀ = 926 nM, plasma concentration: 107 μM, PPB: 99.9%). Compound **29** was efficacious against thermal stimulation at 20 mg kg⁻¹, s.c. The target coverage of **29** in this assay was 1.9-fold. Thus, Merck successfully reproduced the anosmia conditions observed in patients with Nav_v1.7 loss-of-function by inhibiting Nav_v1.7. They also revealed that heat withdrawal responses can be inhibited with lower Nav_v1.7 coverage than odour-induced activation of OB in rhesus monkeys because compound **29** was not efficacious in the OB assay at an Nav_v1.7 coverage of 3.4-fold (2.68 mg kg⁻¹, i.v.) whereas it was efficacious in the thermal assay at 1.9-fold.⁹⁰

Because Nav_v1.6 blockade leads to respiratory inhibition in the phrenic nerve preclinically, Merck identified compound **30** with better Nav_v1.6 selectivity (60-fold). They conducted an *in vitro* evaluation using the hyperpolarised assay protocol, which is close to the resting state. Surprisingly, compound **30** required 0.04-fold Nav_v1.7 coverage in plasma at *in vivo* EC₅₀, whereas 4.8-fold target coverage was required in the rhesus OB assay. Based on these results, the estimated human dose varies from 40 (BID) to 4600 mg (BID), and they concluded that further optimisation was needed to acquire clinical candidates.⁹¹

Bristol-Myers Squibb reported the identification of compound **31**. In their article, both compounds **24** and **31** were assessed for their ability to reduce nociceptive behaviour in a formalin test in mice, revealing that **24** was effective at 60 mg kg⁻¹ whereas **31** was not effective at 100 mg kg⁻¹. The target coverage values of these compounds in plasma were 326- and 43-fold, respectively. They evaluated the DRG concentrations of both compounds, and the concentrations of **24** and **31** reached 0.34 and 0.072 μM, respectively, corresponding to 21- and 0.77-fold target coverage in the DRG, respectively, given the plasma protein

binding as an estimate of tissue binding. They speculated that greater target coverage in the DRG was required for high efficacy and synthesised two compounds exceeding the target coverage by more than 10-fold in the DRG. One compound successfully displayed statistically significant efficacy, whereas another failed to elicit robust efficacy even though both compounds possessed comparable properties, including similar target coverage in the DRG.⁹²

Compound **32** achieved improved membrane permeability by avoiding the zwitterionic characteristics of **31** and better exposure in the DRG. Thus, compound **32** was efficacious in mouse CCI and CFA models at Na_v1.7 coverage values of 14- and 0.5-fold, respectively. Notably, compound **32** was efficacious in the phase 2 mouse formalin model at 1-fold Na_v1.7 coverage in the DRG. They also reported high exposure in the trigeminal ganglion in the mouse formalin model. They confirmed that compound **32** elevated the electrical threshold for the nociceptive flexion reflex to elicit an electromyographic response to the activation of A δ

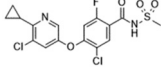
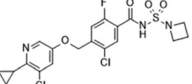
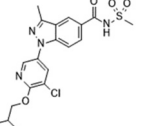
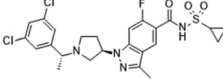
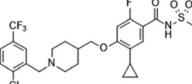
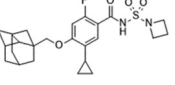
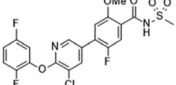
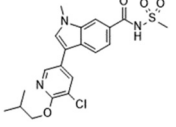
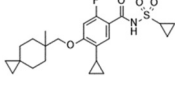
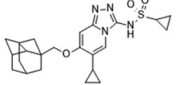
nociceptive neurons in a highly corrected manner with plasma exposure.⁹³

As previously described, almost all sulphonamide derivatives induced potent selective inhibition of hNa_v1.7 and exhibited robust efficacy with high Na_v1.7 coverage in preclinical animal studies. This high target coverage was realised by the enhancement of *in vitro* Na_v1.7 activity. Some compounds are expected to display human efficacy at a lower dose given that efficacy is predicted by the *in vitro* IC₅₀ and human PK parameters. Further, our group reported the excellent preclinical safety profile of DS-1971 (**19**) for the initiation of clinical trials.⁴⁸ The reasons why these attractive clinical candidates did not proceed to clinical trials are discussed in the following section.

7. Acyl sulphonamides

In 2012, Pfizer described the acyl sulphonamide derivatives **33**, **34** and **35** with potent Na_v1.7 inhibitory activity in a patent (Table 8).^{95–97} These observations led to the discovery

Table 8 Acyl sulphonamide derivatives with their *in vitro* profiles and target coverage^a

					
	33: Pfizer ⁹⁵	34: Pfizer ⁹⁶	PF-05241328 (35) ⁹⁷	GX-585 (36) ⁷⁷	GX-201 (37) ⁷⁷
hNa _v 1.1 IC ₅₀	—	—	—	100 nM ^{c,e}	192 nM ^{c,e}
hNa _v 1.5 IC ₅₀	—	—	—	435 nM ^{c,f}	705 nM ^{c,f}
hNa _v 1.7 IC ₅₀	30 nM ^{c,d}	90 nM ^{c,d}	22 nM ^{c,d}	15.1 nM ^{c,f}	3.2 nM ^{c,f}
Mouse Na _v 1.7 IC ₅₀	—	—	—	—	—
Mouse PPB ^b	—	—	—	99.3%	99.8%
Na _v 1.7 coverage in plasma@efficacious dosage ^a	—	—	—	3.4-Fold@ <i>in vivo</i> EC ₅₀ (IEM mouse)	0.61-Fold@ <i>in vivo</i> EC ₅₀ (IEM mouse)
					
	GDC-0276 (38) ⁷⁸	39: Amgen ⁹⁹	40: Bristol-Myers Squibb ⁹⁴	41: Xenon/Genentech ¹⁰⁰	GNE-131 (42) ¹⁰¹
hNa _v 1.1 IC ₅₀	10.6 nM ^{d,g}	8500 nM ^{c,h}	—	6 nM ^{d,g}	45 nM ^{d,g}
hNa _v 1.5 IC ₅₀	51 nM ^{d,g}	11 900 nM ^{c,h}	19 000 nM ^{g,k}	50 nM ^{d,g}	110 nM ^{d,g}
hNa _v 1.7 IC ₅₀	0.4 nM ^{d,g}	51 nM ^{c,h}	8 nM ^{c,l}	0.6 nM ^{d,g}	3 nM ^{d,g}
Mouse Na _v 1.7 IC ₅₀	—	115 nM, 270 nM ⁱ	35 nM ^{c,l} , 11 nM ^{c,l,m}	2.2 nM ^{d,g}	—
Mouse PPB ^b	99.98%	98.6%	99.8%, 96.5% ⁿ	99.9%	99.9%
Na _v 1.7 coverage in plasma@efficacious dosage ^a	1-Fold@ <i>in vivo</i> EC ₅₀ (IEM mouse)	36-Fold@300 mg kg ⁻¹ (15-fold@300 mg kg ^{-1,j}) (mouse histamine)	8.7-Fold@30 mg kg ⁻¹ IP ^o 3.4-Fold@30 mg kg ⁻¹ IP (mouse formalin) 3.6-Fold@30 mg kg ⁻¹ IP (mouse CFA) 3.9-Fold@30 mg kg ⁻¹ IP (mouse CCI)	5-Fold@0.30 mg kg ⁻¹ (IEM mouse) 23-Fold@10 mg kg ⁻¹ (mouse formalin)	0.17-Fold@ <i>in vivo</i> EC ₅₀ (IEM mouse)

^a Na_v1.7 coverage = free plasma concentration/*in vitro* Na_v1.7 IC₅₀. ^b Plasma protein binding. ^c Value in the manual patch-clamp assay. ^d Value in an inactivated state. ^e Value at V_{hold} = -45 mV. ^f Value at V_{hold} = -60 mV. ^g Value in the automated patch-clamp assay. ^h Value at a voltage yielding 20% channel inactivation. ⁱ IC₅₀ of native TTX-S currents in the mouse DRG. ^j Calculated from the mouse TTX-S IC₅₀. ^k Value at V_{hold} = -50 mV. ^l Value at V_{hold} = -70 mV. ^m IC₅₀ of mouse DRG Na_v1.7. ⁿ Value in the mouse DRG. ^o Na_v1.7 coverage in the DRG: free DRG concentration/*in vitro* IC₅₀ of mouse DRG Na_v1.7.

of GX-585 (**36**) and GX-201 (**37**), as reported by Xenon/Genentech. Compounds **36** and **37** inhibited hNa_v1.7 with IC₅₀ values of 15.1 and 3.2 nM, respectively, and they were efficacious in IEM transgenic mice. The *in vivo* IC₅₀ values of **36** and **37** were 7.3 and 0.97 μM, respectively, and their target coverage values were 3.4- and 0.61-fold, respectively. They reported the target coverage for sulphonamide derivatives, including PF-05089771 (**16**) and compound **24** (Table 7), which required coverage of 82- and 28-fold, respectively, for significant efficacy in their animal model. Acyl sulphonamides **36** and **37** required less target coverage to induce robust efficacy *in vivo* than the sulphonamides **16** and **24**. Because **36** and **37** displayed longer residence times than **16** and **24**, they concluded that the improved *in vivo* efficacy was correlated with extremely slow dissociation from Na_v1.7. They reported the efficacy of the compounds in various *in vivo* models of neuropathic and inflammatory pain. A radioligand study illustrated that **36** and **37** bonded competitively to VSD4, the same binding site used by sulphonamide derivatives.⁷⁷

The adamantane derivative GDC-0276 (**38**) was disclosed by Genentech. A preclinical *in vivo* study of GDC-0276 was conducted using IEM transgenic mice. At the *in vivo* EC₅₀ of 1.7 μM, the target coverage of **38** was 1-fold, which aligned with their conclusion that this low target coverage is sufficient for robust efficacy in acyl sulphonamides.⁷⁸ Compound **16** (Table 6) displayed poor *in vivo* efficacy with EC₅₀ > 18 μM in their *in vivo* assay. Although phase 1 clinical trials of both GDC-0276 and GDC-0310 were completed, the development of both compounds was terminated.^{78,98}

Amgen disclosed biphenyl acyl sulphonamide derivative **39**. A PK/PD study in a mouse histamine-induced scratching model demonstrated a robust reduction of scratching bouts at a dose of 300 mg kg⁻¹, p.o. The unbound plasma concentration (C_u plasma = 4.15 μM) was more than 15-fold greater than the IC₅₀ measured on native TTX-S currents in mouse DRG neurons (IC₅₀ = 0.27 μM) at 300 mg kg⁻¹.⁹⁹ In comparison to another Na_v1.7 inhibitor, the Na_v1.7 coverage of which was calculated at the mNa_v1.7 IC₅₀, the Na_v1.7 coverage of **39** was calculated as 36-fold (mNa_v1.7 IC₅₀ = 115 nM).

Bristol-Myers Squibb discovered the indole **40**, which inhibited hNa_v1.7 at an IC₅₀ of 8 nM with excellent subtype selectivity over hNa_v1.5. **40** was efficacious in the reversal of phase 2 formalin-induced nociceptive behaviours in mice at 30 mg kg⁻¹ IP. At 30 mg kg⁻¹ IP, compound **40** reversed the nociceptive behaviours to normal levels. Na_v1.7 coverage in the DRG (free DRG concentration/*in vitro* IC₅₀ of mouse DRG Na_v1.7) was 8.7-fold, whereas Na_v1.7 coverage in plasma was 3.4-fold higher than the mNa_v1.7 IC₅₀. The reference compound **24** (Table 7) reversed phase 2 formalin-induced nociceptive behaviour to normal levels at 30 mg kg⁻¹, p.o., at which the target coverage in the DRG was 189-fold, and the coverage in plasma reached 87-fold. A close analogue of **40** that achieved a target coverage of 5.5-fold in

the DRG (the target coverage in plasma: 5.4-fold) failed to display efficacy in the formalin model. Because the subtype selectivity, PK profile, off-target activity and binding kinetics of active and inactive compounds were identical, they concluded that a small difference in target coverage in the mouse DRG (8.7-fold vs. 5.5-fold) led to a significant difference in *in vivo* efficacy. Although a lower dose of **24** was not examined, it could be concluded that **24** needed higher target coverage than **40** for high efficacy *in vivo*. Compound **40** was reported to be significantly efficacious in the mouse CFA model of inflammatory pain at 30 mg kg⁻¹ IP, whereas the effect was modest against cold allodynia in the mouse CCI model at 30 mg kg⁻¹ IP. The target coverage values in the CFA and CCI assays were 3.6- and 3.9-fold in plasma, respectively. Sural fascicle recording studies illustrated that **40** and a close analogue were efficacious against mechanosensitivity of the mouse sural nerve at a dose of 30 mg kg⁻¹ IP, whereas only **40** was efficacious against mechanosensitivity of the mouse sural nerve when the compound was applied directly to the nerve at 100 μM.⁹⁴

Xenon/Genentech disclosed the highly potent acyl sulphonamide **41**. Compound **41** inhibited both hNa_v1.7 at IC₅₀ = 0.6 nM and rat orthologues (IC₅₀ = 3.7 nM), whereas an *in vivo* evaluation of **38** was performed in mice. Compound **41** was efficacious in aconitine-induced pain in IEM transgenic mice from 0.3 mg kg⁻¹, p.o. The plasma concentration of **41** was approximately 3.1 μM at a dose of 0.3 mg kg⁻¹ (unbound plasma concentration: 3 nM), which is approximately 5-fold higher than the hNa_v1.7 IC₅₀. Compound **41** exerted a significant effect in the phase 2 formalin assay at 10 mg kg⁻¹, p.o. The plasma concentration of **41** was 50 μM, which corresponded to 23-fold target coverage in plasma.¹⁰⁰

GNE-131 (**42**) is a less selective acyl sulphonamide that inhibited hNa_v1.7 (IC₅₀ = 3 nM). GNE-131 was efficacious in a mouse IEM model from 10 mg kg⁻¹, and the *in vivo* EC₅₀ was determined as 0.5 μM via two-point sigmoid calculation, which corresponded to hNa_v1.7 coverage of 0.17-fold. Notably, they reported the discrepancy between *in vivo* efficacy and *in vitro* potency for their close analogues.¹⁰¹

Acyl sulphonamide derivatives possess higher plasma binding ability than sulphonamides owing to the higher acidity of the acyl sulphonamide group. As mentioned by the Xenon/Genentech group, acyl sulphonamides tend to demonstrate robust efficacy with lower target coverage than sulphonamides.^{77,78} As acyl sulphonamides exhibited less subtype selectivity than sulphonamides, this suggested the possible contribution of other VGSCs to the effects. It should be noticed that the less subtype-selective compound GNE-131 (**42**) elicited efficacy in IEM mice at low Na_v1.7 coverage (0.17-fold).

Although the preclinical safety profile of acyl sulphonamides has not been disclosed to date, the acyl sulphonamide GDC-0276 (**38**) exhibited higher toxicity than PF-05089771, which is discussed in the following section.^{78,98}

8. Pharmacological effects of Na_v1.7 inhibitors in *in vivo* animal models

Animal experiments are inevitable in the research and development of analgesics, and various types of *in vivo* experimental animal models have been used to evaluate the pharmacological effects of Na_v1.7 inhibitors. Some examples of animal models used for the pharmacological evaluation of Na_v1.7 inhibitors are listed in Table 9. Although traditional nociceptive and NP models with various stimulation methods (*e.g.*, chemical, mechanical, thermal, cold, electrical) have been widely used, it appears that each pharmaceutical company has developed a unique research strategy for the *in vivo* screening of Na_v1.7 inhibitors.

Convergence/Biogen reported that their clinical compound vixotrigine (**6**, Table 6) displayed significant analgesic effects in the CCI and CFA models of rats at doses that did not induce sedation or ataxia.⁵⁷ PF-05089771 (**16**, Table 7), a clinical compound developed by Pfizer/Icagen, is a

breakthrough compound exhibiting potent and selective Na_v1.7 inhibition, and its *in vitro* effects were described in several peer-reviewed papers.^{73–75,102,103} Although Pfizer/Icagen have not published the results of *in vivo* pharmacological studies of PF-05089771, their patent mentioned the synergic analgesic effects of analogues of **16** and pregabalin in the mouse formalin test.¹⁰⁴ Pfizer/Icagen's non-clinical tool compound PF-05198007 inhibited capsaicin-induced flare response and capsaicin-induced nociceptive behaviour in mice,^{75,105} whereas another tool compound named PF-06456384 exerted no significant analgesic effects in the mouse formalin test.⁸⁹

Generally, the evaluation of the effects of drugs on mechanical hypersensitivity (*i.e.*, allodynia, hyperalgesia) using the von Frey test is regarded as the gold standard for *in vivo* screening in NP models. However, we found that Na_v1.7 inhibitors are more effective against thermal hypersensitivity than mechanical hypersensitivity in NP models and screened a series of Na_v1.7 inhibitors using a thermal assay (Hargreaves test) in PSNL model mice.^{47,48} As a

Table 9 Animal models used in the evaluation of Na_v1.7 inhibitors

Category	Model	Endpoint	Species	Ref.
Pain (nociceptive model)	Hot plate	Nociceptive response (hind paw flinching/licking) induced by noxious thermal stimuli	Mouse	77
	Heat thermode	Nociceptive response (forearm withdrawal) induced by noxious thermal stimuli	Rhesus monkey	90
	Acetic acid	Nociceptive response (abdominal writhing) induced by the intraperitoneal injection of acetic acid	Mouse	111
	Formalin	Nociceptive response (hind paw flinching/licking/lifting) induced by the intraplantar injection of formalin	Mouse/rat	69, 70, 77, 80, 84, 85, 86, 90, 101
	Capsaicin	Nociceptive response (hind paw licking) induced by the intraplantar injection of capsaicin	Mouse	86
	CFA	Mechanical hypersensitivity induced by the intraplantar injection of CFA Thermal hypersensitivity induced by the intraplantar injection of CFA Cold hypersensitivity induced by the intraplantar injection of CFA	Rat Mouse/rat Mouse	57, 68 61, 82, 112 77, 79
	MIA	Grip force deficit of hind limbs induced by intra-articular knee injection of MIA	Rat	63
Pain (neuropathic model)	Ultraviolet-B (UVB)	Thermal hypersensitivity induced by UVB irradiation to the hind paw	Mouse	86
	STZ-induced diabetes	Mechanical hypersensitivity induced by diabetic neuropathy	Mouse	77
	CCI	Mechanical hypersensitivity induced by CCI	Rat	57
	SNL	Mechanical hypersensitivity induced by SNL	Mouse/rat	48, 61, 62, 67, 68
	PSNL	Mechanical hypersensitivity induced by PSNL Thermal hypersensitivity induced by PSNL	Mouse Mouse	48 47, 48
Pain (target engagement model)	Spared nerve injury (SNI)	Cold hypersensitivity induced by SNI	Mouse	77
	Scorpion toxin OD1	Nociceptive response (hind paw licking/flinching/lifting/shaking) induced by the intraplantar injection of OD1	Mouse	58
	Aconitine	Nociceptive response (hind paw flinching) induced by the intraplantar injection of aconitine in normal mice	Rat	79
	IEM-aconitine	Nociceptive response (hind paw flinching/licking/biting) induced by the intraplantar injection of aconitine in IEM transgenic mice	Mouse	77, 78, 82, 100, 101
Others	Itch	Scratching behaviour induced by the intradermal injection of histamine into the neck	Mouse	83, 85, 86, 99
	Cough	Coughing response induced by citric acid inhalation	Guinea pig	109
	Skin blood flow	Flare response induced by the topical skin application of capsaicin	Mouse	75
	Olfactory fMRI	Olfaction response (fMRI signal) in OB induced by odour stimulation	Rhesus monkey	90

result, we obtained DS-1971a (**19**, Table 7), a clinical compound, exerting a potent analgesic effect on thermal hypersensitivity in PSNL model mice with an ED_{50} of 0.32 mg kg^{-1} , p.o., making it more potent than PF-05089771 (ED_{50} = 3.0 mg kg^{-1} , p.o.). DS-1971a also significantly inhibited mechanical hypersensitivity in PSNL and SNL model mice at oral doses of at least 1 mg kg^{-1} .⁴⁸ Amgen's research group adopted histamine-induced scratching behaviour in mice (*i.e.*, antipruritic activity) to screen their $Na_V1.7$ inhibitors, including small molecules,^{81,83,86–88,100} peptides¹⁰⁶ and antibodies,¹⁰⁷ based on the findings from phenotype analyses of $Na_V1.7$ knockout mice.¹² Xenon/Genentech reported a target engagement assay of aconitine-induced nociceptive behaviour in IEM transgenic mice.^{77,82,100,101} The IEM transgenic mice displayed enhanced nociceptive responses (flinching and licking of the hind paws) elicited by the intraplantar injection of aconitine, a Na_V activator, compared to the findings in wild-type mice.⁷⁷ Their clinical compounds, namely GDC-0276 and GDC-0310, exerted dose-dependent analgesic effects at lower plasma concentrations than PF-05089771.⁷⁸ Another target engagement assay using the scorpion toxin OD1, a $Na_V1.7$ activator, was also reported. Vixotrigine and PF-04856264, an aryl sulphonamide, inhibited nociceptive responses evoked by the intraplantar injection of OD1.⁵⁸

Concerning sulphonamides and acyl sulphonamides, large species differences in $Na_V1.7$ blockade make the choice and interpretation of animal experiments more difficult. For instance, PF-05089771 was found to be far less potent against rat $Na_V1.7$ than against human, mouse, dog and cynomolgus macaque $Na_V1.7$.^{73,75} Namely, rats, as the most commonly used species in preclinical studies, are not appropriate for evaluating the pharmacological effects of sulphonamides and acyl sulphonamides. Therefore, many pharmaceutical companies have used mice in preclinical pharmacodynamic studies of sulphonamides and acyl sulphonamides.^{48,77,78,80–89,91–94,99–101} Lilly and their collaborators reported the antitussive effects of compound 801, a sulphonamide-based $Na_V1.7$ inhibitor, on citric acid-evoked coughing in guinea pigs.^{108,109} Recently, Merck reported a battery of four translational assays using rhesus monkeys: 1) microneurography for the action potential propagation in unmyelinated afferents, 2) threshold tracking for the excitability of myelinated afferents, 3) heat nociception test using clinical thermode device and 4) functional magnetic resonance imaging (fMRI) for olfactory function. Their sulphonamides exerted dose-dependent and significant effects in microneurography, heat nociception and fMRI assays.⁹⁰ These assays provide back-translation from clinical examination to preclinical research with non-human primates.¹¹⁰ It is expected that they could be used as pharmacodynamic endpoints for $Na_V1.7$ inhibitors in clinical trials.

In addition to the aforementioned analgesic and/or antipruritic effects of $Na_V1.7$ inhibitors, their side effect profiles have been published. It is notable that no sulphonamide-based $Na_V1.7$ inhibitors exerted significant side effects on the CNS and CV system.^{48,77,86} This is one of the most remarkable

aspects of selective $Na_V1.7$ inhibitors and a major differentiation point *versus* non-selective VGSC inhibitors.

9. Clinical studies of $Na_V1.7$ inhibitors

Many investigators including academic, biotech and mega pharma companies have been conducting research and development on selective $Na_V1.7$ inhibitors. However, no group has successfully developed and launched a $Na_V1.7$ inhibitor to date. Clinical trials of $Na_V1.7$ inhibitors are listed in Table 10.

Vixotrigine (**6**, Table 6) is a current front-runner in the development of selective $Na_V1.7$ inhibitors. Although compound **6** was initially reported as a selective $Na_V1.7$ inhibitor, recent studies demonstrated that it is neither selective nor potent.^{46,56,58} Some phase 2 trials of forms of NP, such as trigeminal neuralgia, lumbosacral radiculopathy and small fibre neuropathy, were completed with mixed results. The detailed study design and outcomes of a phase 2a randomised withdrawal trial in trigeminal neuralgia have been published.^{113,114} Although the criterion for the primary endpoint of treatment failure was not met (33% treatment failure for vixotrigine 150 mg TID, 64% treatment failure for placebo, $p = 0.0974$), significant efficacy trends in the secondary endpoints (*e.g.*, average daily pain score, number and severity of paroxysms) indicated the considerable potential for this compound in the treatment of trigeminal neuralgia.¹¹⁴ Two phase 3 trials in trigeminal neuralgia are planned, but recruitment has not commenced as of 2021.⁵⁹

Funapide (**5**, Table 6) is considered a non-selective VGSC inhibitor.⁵⁵ Oral administration of funapide (400 mg BID) produced analgesic effects in an exploratory clinical study of four patients with IEM, a gain-of-function mutation of $Na_V1.7$.¹¹⁵ Subsequently, the compound was developed as a topical ointment to reduce systemic drug exposure and related adverse events, but phase 2 trials in postherpetic neuralgia (PHN) and knee OA failed to meet the primary endpoints (NCT02068599, NCT02365636). However, the result of subpopulation analysis in a phase 2a proof-of-concept study for PHN was worthy of notice. Patients with PHN carrying the R1150W polymorphism (arginine to tryptophan substitution at 1150), a gain-of-function $Na_V1.7$ variant, exhibited more marked analgesic responses to funapide ointment than wild-type carriers.¹¹⁶ Recently, Flexion Therapeutics initiated a phase 1 trial in post-surgical pain patients undergoing bunionectomy using a thermosensitive extended-release hydrogel formulation.

Pfizer/Icagen's compound PF-05089771 (**16**, Table 7) is an epoch-making compound exhibiting potent and selective $Na_V1.7$ blocking activity,^{73,74} and their development strategy and approach were informative and suggestive. Pfizer conducted an exploratory clinical micro-dosing study to investigate the intravenous and oral pharmacokinetic profile of four compounds (PF-05089771, PF-05150122, PF-05186462 and PF-05241328) and selected PF-05089771 as a clinical candidate (NCT01165736).¹¹⁷ In a phase 1 single ascending

Table 10 Clinical trials of Na_v1.7 inhibitors

Compound [sponsor]	Condition/indication	Study		Identifier ^a	Ref.
		phase	Study status		
Vixotrigine/raxatrigine/BIIB074/CNV1014802/GSK1014802 [Biogen/Convergence/GlaxoSmithKline]	HV (SD, resting motor threshold)	1	Completed 2008	NCT00488566	113,
	HV (MD)	1	Completed 2008	NCT00908154	114
	HV (SD, electrical stimulation)	1	Terminated 2009	NCT00964288	
	HV (MD, ambulatory blood pressure)	1	Completed 2009	NCT00955396	
	Lumbosacral radiculopathy (MD)	2	Completed 2012	NCT01561027	
	Trigeminal neuralgia (MD)	2a	Completed 2014	NCT01540630	
	HV (MD, age, gender)	1	Completed 2015	NCT02359344	
	HV (MD, DDI)	1	Completed 2016	NCT02551497	
	HV (MD, DDI)	1	Completed 2016	NCT02698267	
	HV (SD, hot ADME)	1	Completed 2016	NCT02751905	
	IEM (MD)	2a	Completed 2017	NCT02917187	
	HV (SD, MD, race)	1	Completed 2017	NCT02831517	
	HV (SD, RBA)	1	Completed 2017	NCT02951221	
	HV (MD, DDI)	1	Completed 2017	NCT03385525	
	HV (MD, DDI)	1	Completed 2018	NCT03324685	
	Lumbosacral radiculopathy (MD)	2	Completed 2018	NCT02935608	
	Lumbosacral radiculopathy (MD)	2	Terminated 2019	NCT02957617	
	Small fibre neuropathy (MD)	2	Terminated 2021	NCT03339336	
	Trigeminal neuralgia (MD)	3	Not yet recruiting 2021	NCT03070132	59
	Trigeminal neuralgia (MD)	3	Not yet recruiting 2021	NCT03637387	59
Funapide/XEN402/XPF-002/TV-45070/FX301 [Xenon/Teva/Flexion]	IEM (MD, oral)	2a	Completed 2010	NCT01090622	115
	PHN (MD, ointment)	2a	Completed 2011	NCT01195636	116
	IEM (MD, ointment)	2a	Completed 2012	NCT01486446	
	HV (MD, ointment)	1	Completed 2015	NCT02215941	
	Knee osteoarthritis (MD, ointment)	2	Completed 2015	NCT02068599	
	PHN (MD, ointment)	2	Completed 2017	NCT02365636	
PF-05089771 [Pfizer/Icagen]	Postoperative pain (SD, local injection)	1	Recruiting 2021	NCT04826328	
	HV (SD, micro-dosing, oral and intravenous)	1	Completed 2010	NCT01165736	117
	HV (SD, exploratory pharmacodynamics)	1	Completed 2011	NCT01259882	
	HV (MD)	1	Completed 2011	NCT01365637	
	HV (SD, RBA)	1	Completed 2012	NCT01563497	
Postoperative dental pain (SD)	2	Completed 2012	NCT01529346		

Table 10 (continued)

Compound [sponsor]	Condition/indication	Study phase	Study status	Identifier ^a	Ref.
AZD3161 [AstraZeneca]	HV (SD, RBA)	1	Completed 2012	NCT01690351	
	HV and knee OA (MD)	1	Completed 2012	NCT01529671	
	HV (MD, titration)	1	Completed 2013	NCT01772264	
	IEM (SD)	2	Completed 2013	NCT01769274	
	HV (SD, RBA)	1	Completed 2013	NCT01854996	
	HV (SD, MD, DDI)	1	Completed 2013	NCT01934569	
	HV (SD, pain model)	1	Completed 2015	NCT02349607	118
	Diabetic peripheral neuropathy (MD)	2	Completed 2015	NCT02215252	119
	HV (SD, UVC, intradermal injection)	1	Completed 2011	NCT01240148	
	DSP-2230 [Sumitomo Dainippon/Sunovion]	HV (SD, MD, RBA)	1	Completed 2013	ISRCTN07951717
HV (SD, capsaicin and UVB)		1	Completed 2013	ISRCTN80154838	
HV (MD, renal function)		1	Completed 2013	ISRCTN02543559	
DS-1971a [Daiichi Sankyo]	HV (SD)	1	Completed 2014	NCT02107885	
	HV (MD)	1	Completed 2014	NCT02190058	
	HV (SD, age, gender, race)	1	Completed 2014	NCT02261376	
	HV (SD, RBA)	1	Completed 2015	NCT02266940	
	HV (MD, DDI)	1	Completed 2015	NCT02473627	
	HV (MD, gender)	1	Completed 2015	NCT02564861	
	Diabetic PNMD)	2	Withdrawn 2016	NCT02673866	
GDC-0276/RG7893 [Xenon/Genentech/Roche]	Radiculopathy attributable to LSS (MD)	2	Withdrawn 2016	JapicCTI-163 193	
	HV (SD, RBA)	1	Withdrawn 2016	NCT02856152	98
GDC-0310/RG6029 [Xenon/Genentech/Roche]	HV (SD, MD, RBA)	1	Completed 2017	NCT02742779	
BIIB095 [Biogen/Convergence]	HV (SD, MD)	1	Completed 2019	NCT03454126	
	HV and diabetic peripheral neuropathy	1b	Withdrawn 2021	NCT04106050	
CC8464/APS1807 [Chromocell/Astellas]	HV (SD, MD, RBA, DDI)	1	Completed	Not registered	
DSP-3905 [Sumitomo Dainippon/Sunovion]	HV	1	Not disclosed	Not registered	

^a From ClinicalTrials.gov (<https://clinicaltrials.gov/ct2/home>), ISRCTN registry (<https://www.isrctn.com/>) and Japic Clinical Trials Information (<https://www.clinicaltrials.jp/cti-user/common/Top.jsp>). HV, healthy volunteer; SD, single dose; MD, multiple dose; RBA, relative bioavailability; DDI, drug–drug interaction.

dose study of PF-05089771, exploratory pharmacodynamic parameters such as the heat pain perception threshold and odour threshold (Sniffin' Sticks) were investigated in healthy subjects, but the results have not been disclosed (NCT01259882). In another phase 1 trial for pharmacodynamic evaluation, a single oral dose of PF-05089771 (300 mg) produced no significant analgesic effects

in a battery of human evoked pain models (PainCart test). Namely, PF-05089771 alone or concomitantly with pregabalin had no effects on the heat pain detection threshold under normal and UVB-exposed skin conditions and pain tolerance to electrical, pressure and cold pressor stimulation in healthy subjects (NCT02349607).¹¹⁸ In phase 1 multiple-dose studies, skin rash observed at oral doses of 450 and 600 mg BID was

determined as the dose-limiting adverse effect (NCT01365637, NCT01529671). Therefore, an additional phase 1 trial with a 4 week titration regimen was conducted to reduce the incidence of skin rash (NCT01772264). Although the results of the additional phase 1 trial have not been disclosed, the 4 week titration regimen might not have been effective. In fact, the maximum dose was set at 150 mg BID without titration in the last phase 2 trial for patients with diabetic peripheral neuropathy because of the potential for drug–drug interactions and cholesterol elevation (NCT02215252).¹¹⁹ Phase 2 trials of PF-05089771 were conducted in three pathological pain states (*i.e.*, postoperative dental pain, IEM, diabetic peripheral neuropathy). In a phase 2 trial for postoperative dental pain (NCT01529346), PF-05089771 (150, 450 and 1600 mg) significantly reduced pain, but its efficacy was far inferior to that of ibuprofen (400 mg). On the contrary, a single oral dose of PF-05089771 (1600 mg) produced analgesic effects in a phase 2 trial of five patients with IEM (NCT01769274), and the compound inhibited the hyperexcitability of iPSC-derived sensory neurons from patients with IEM in *in vitro* electrophysiological experiments.¹⁰² The results of a phase 2 trial in diabetic peripheral neuropathy have been published.¹¹⁹ PF-05089771 (150 mg BID, 4 weeks) was well tolerated, and a trend towards efficacy was noted (a decrease in the weekly average pain score). However, the effect was weaker than that of pregabalin (150 mg BID) and not statistically significant *versus* placebo at 4 weeks. For treatment-related adverse events, total and LDL cholesterol elevation was observed, but skin rash and CV- or CNS-related adverse events were not observed in this trial. It is interesting to note that the results of the primary analysis were somewhat different from those of the sensitivity analysis (mixed-model repeated-measures analysis). In the results of the primary analysis registered on <https://ClinicalTrials.gov>, the time-course changes in the weekly average pain score of the PF-05089771 treatment group were almost identical to those of the pregabalin treatment group (NCT02215252). The aforementioned outcomes of the three phase 2 trials suggest that the appropriate target indication for selective Na_v1.7 inhibitors is NP rather than nociceptive pain. At present, PF-05089771 cannot be found in Pfizer's pipeline.

Daiichi Sankyo's sulphonamide derivative DS-1971a (19, Table 7) is a potent and selective Na_v1.7 inhibitor with a favourable pharmacological and toxicological profile.⁴⁸ A series of phase 1 trials of DS-1971a were successfully completed, and its favourable safety profile was confirmed. DS-1971a exhibited good safety and tolerability up to 1500 mg in a single ascending dose study (NCT02107885) and up to 1200 mg per day (600 mg BID or 400 mg TID) in a 14 day multiple-dose study (NCT02190058). In contrast to PF-05089771, skin rash or cholesterol elevation was not observed in any phase 1 trials. Two phase 2 trials for peripheral NP (*i.e.*, diabetic peripheral neuropathy, radiculopathy attributable to lumbar spinal stenosis) had been planned

(NCT02673866, JapicCTI-163193), but both trials were terminated immediately before initiation because of toxicological findings in long-term toxicity studies in rats. Daiichi Sankyo has decided to discontinue the development programme of this compound.

Although several other Na_v1.7 inhibitors have been found on clinical trial databases and corporate websites, their development statuses have not been updated, and some of them have already disappeared from their companies' pipelines.

AstraZeneca completed a phase 1 trial of AZD3161 (7, Table 6) in 2011 that assessed the effects of intradermal AZD3161 on quantitative sensory testing in normal and UVC-exposed skin in healthy subjects (NCT01240148). However, the study results have not been disclosed, and the compound has disappeared from the company's pipeline.

Sumitomo Dainippon/Sunovion completed three phase trials of DSP-2230, a Na_v1.7/1.8 dual inhibitor, in 2013 (ISRCTN07951717, ISRCTN80154838, ISRCTN02543559). The study results have not been disclosed, and the compound has disappeared from their pipeline. Although Sumitomo Dainippon and Sunovion have also mentioned DSP-3905, a selective Na_v1.7 inhibitor, on their websites, the detailed information of this compound has not been disclosed.

Genentech completed two phase 1 trials of GDC-0276/RG7893 (38, Table 8; NCT02856152) and GDC-0310/RG6029 (NCT02742779) in 2016 and 2017, respectively, and discontinued their subsequent development.⁷⁸ The detailed results of phase 1 trial for GDC-0276/RG7893 were published, and various adverse events such as liver transaminase elevation, diarrhoea, dizziness and hypotension were observed in the treatment groups.⁹⁸

Two phase 1 trials of BIIB095 (Biogen/Convergence) were registered on <https://ClinicalTrials.gov> (NCT03454126, NCT04106050), but this compound is no longer present in Biogen's pipeline.

Chromocell/Astellas announced that the FDA granted fast track designation to their candidate compound CC8464/ASP1807 for idiopathic small fibre neuropathy in October 2016.¹²⁰ Although they completed a series of phase 1 trials of CC8464/ASP1807, Astellas announced the discontinuation of the research and development programme of CC8464/ASP1807 in January 2019.

10. Discussion

10.1. The relationship between *in vivo* efficacy and Na_v1.7 coverage among three types of VGSC inhibitors

Conventional VGSC inhibitors exhibit efficacy in preclinical studies with less target coverage than sulphonamides or acyl sulphonamides. In the formalin model, compounds 14 (0.25-fold) and 15 (0.035-fold) elicited statistically significant efficacy at target coverage values of less than 1, whereas at least several folds of target coverage were required for sulphonamides 17 (10-fold), 18 (10-fold), 22 (1.3-fold in rats, 10-fold in mice), 23 (100-fold), 24 (11, 87, 326-fold) and 32

(3-fold) and acyl sulphonamides **40** (3.4-fold) and **41** (23-fold). In IEM mice, sulphonamides **16** (82-fold), **21** (25-fold) and **24** (28-fold) required higher $\text{Na}_v1.7$ coverage than acyl sulphonamides **36** (3.4-fold), **37** (0.61-fold), **38** (1-fold), **41** (5-fold) and **42** (0.17-fold). This observation is aligned with the conclusion of Xenon/Genentech.^{77,78} The exception is sulphonamides **19** (0.058-fold), **30** (0.04-fold) and **32** (0.5-fold), which displayed statistically significant efficacy at target coverage values of less than 1-fold. In particular, sulphonamide **30** was effective in a mouse formalin model at 0.04-fold target coverage. As the *in vitro* potency of compound **30** was evaluated near the resting state, high *in vitro* potency in the resting state may be related to high *in vivo* efficacy. Different animal models were used in the evaluation of **19**, **30** and **32** (**19**, thermal hyperalgesia in PSNL mice; **30**, mouse formalin; **32**, mouse CFA model). Although such exceptions are acknowledged, it is fair to conclude that sulphonamides require higher target coverage than acyl sulphonamides, whereas conventional VGSC inhibitors require the lowest target coverage. It is interesting that the subtype selectivity decreases in the same order, suggesting the possibility that other VGSC subtypes contribute to the effects or indicating synergic effects. However, the reasons for the higher required target coverage for sulphonamides or acyl sulphonamides remain unclear.

10.2. DRG concentration

Some groups disclosed the target coverage in the DRG, and the measurement of drug concentrations in the DRG may not solve the PK/PD discrepancy, as Bristol-Myers Squibb reported that compounds with similar target coverage in the DRG displayed completely different efficacy in the same *in vivo* model.⁹² It should be noted that the same company concluded that a small difference in target coverage in the mouse DRG (8.7- and 5.5-fold) may cause a significant difference in *in vivo* efficacy. The fact that only compound **40** was efficacious against mechanosensitivity in a mouse sural nerve when the compounds were applied directly to the nerve was a critical observation for solving the PK/PD discrepancy.⁹⁴ As reported by Xenon/Genentech, the possibility of increased partitioning in DRG membranes opposed to the DRG itself should not be ignored for highly lipophilic compounds.¹⁰¹ Hence, although exposure in the DRG is important for *in vivo* efficacy, the measurement of DRG coverage does not always solve the PK/PD discrepancy.

10.3. Residence time

In addition to the IC_{50} , the residence time for a target protein is suggested to be an important factor that determines the pharmacological effects *in vivo*.¹²¹ A comparative study with acyl sulphonamides and aryl sulphonamides revealed that the long residence time of $\text{Na}_v1.7$ inhibitors likely contributes to their superior analgesic effects *in vivo*. Furthermore, the analgesic effects of acyl sulphonamides were dramatically enhanced by repeated dosing in a mouse

chronic pain model without drug accumulation in plasma.⁷⁷ These results indicate that continuous inhibition of $\text{Na}_v1.7$ currents induced by a compound with a long residence time results in a potent analgesic effect *in vivo*. In fact, DS-1971, possessing a longer residence time than mexiletine, exerted a potent analgesic effect in NP model mice at a lower target coverage.⁴⁸

As a long residence time in $\text{Na}_v1.7$ and repeated dosing *in vivo* can contribute to potent efficacy, a longer duration in plasma or the target tissues may contribute to potent efficacy. As discussed by the Xenon/Genentech group,¹⁰¹ compounds with sharp PK profiles (high blood level peaks) would contribute to *in vivo* efficacy less than compounds without sharp PK peaks because of the lower accumulation of the latter compounds. Thus, the time above the IC_{50} considering the unbound fraction could be an important factor for the discussion of *in vivo* efficacy. Further studies are essential to clarify the relationship between the PK curve shape and *in vivo* efficacy by developing multiple chemical scaffolds.

10.4. *In vitro* assay protocol

Sulphonamides and acyl sulphonamides inhibit $\text{Na}_v1.7$ in a state-dependent manner. They exert inhibitory activity by preferably binding to and stabilising the inactivated state of $\text{Na}_v1.7$, whereas the inhibitory activity (IC_{50}) is diminished in the resting state. Conversely, it is difficult to predict the certain state of $\text{Na}_v1.7$ *in vivo*. A plausible solution is discovering compounds with high potency in the resting state, enabling compounds to bind and stabilise all states of $\text{Na}_v1.7$ because inhibition in the resting state enables the retention of inhibitory activity in both inactivated and open states. In fact, compound **30** reported by Merck inhibited $\text{Na}_v1.7$ in a conformation close to the resting state and demonstrated potent *in vivo* efficacy at extremely low $\text{Na}_v1.7$ coverage (0.04-fold).⁹¹ Janssen reported a close relationship between the $\text{Na}_v1.7$ resting state and pharmacological insensitivity to pain through the identification of the peptide JNJ63955918.¹²² Both cases may approximate the pathological condition observed in patients with CIP. As it is essential for humans to respond to a stimulus with a certain threshold to avoid dangerous signals, this condition is an adverse event in patients with CIP. However, it is possible to avoid such adverse events *via* proper dose setting. Therefore, research to develop compounds that inhibit $\text{Na}_v1.7$ in the resting state could overcome this PK/PD discrepancy. If the current landscape is considered, less toxic sulphonamides with activity in the resting state may be the first target.

10.5. The complexity of *in vivo* models

Pain signals are transmitted from the PNS to the CNS, and the final behavioural decision is made by the CNS. Almost all *in vivo* models for evaluating analgesic agents are based on animal behaviour, and the final behavioural decision is made by the CNS. Therefore, the CNS may contribute to the PK/PD discrepancy to some extent even though the effect of $\text{Na}_v1.7$

is restricted in the PNS.¹²³ The PK/PD discrepancy may be caused by multiple reasons, and many MOAs targeting the CNS face the same problems. Further studies among multiple targets are needed. To connect this PK/PD discrepancy in animal models and humans, further translational research and the development of biomarkers have been awaited.

11. Conclusions

We reviewed three categories of Na_v1.7 inhibitors, namely conventional VGSC inhibitors, sulphonamides and acyl sulphonamides, combined with their background, history, assay technology and assay protocol. Conventional VGSC inhibitors are generally non-selective, and their inhibitory potency is in the micromolar range. Based on these characteristics, these conventional inhibitors displayed the lowest Na_v1.7 coverage at efficacious *in vivo* plasma concentrations among the three categories. The target coverage is usually less than 1-fold. One plausible reason for the low target coverage may be the synergic effects of inhibiting multiple ion channels. If these inhibitors exhibit a sufficient safety margin, they have the potential to be novel analgesic agents. Sulphonamide derivatives, which were first disclosed by Pfizer, induced potent selective Na_v1.7 inhibition *in vitro*, but their *in vivo* efficacy in preclinical studies was generally poor given their high target coverage requirements. Conversely, acyl sulphonamide derivatives tend to require lower target coverage than sulphonamide derivatives to achieve robust *in vivo* efficacy. Thus, the required target coverage increases in the order of sulphonamides, acyl sulphonamides and conventional VGSC inhibitors, and the subtype selectivity decreases in the same order.

Although a clear solution for resolving the PK/PD discrepancy cannot be addressed in this review, we propose the following points for consideration to acquire clinical candidates with robust efficacy by overcoming the PK/PD disconnection: 1) longer residence time in Na_v1.7 *in vitro*, 2) potent inhibitory activity in the resting state *in vitro*, 3) longer duration in plasma (longer duration above the IC₅₀ considering the free fraction), 4) proper selection of the target indication based on the preclinical study and 5) the utilisation of sulphonamides.

We believe continuous research and development of novel Na_v1.7 inhibitors are essential for launching novel analgesic agents.

Abbreviations used

Na _v	Voltage-gated sodium channel
NSAID	Non-steroidal anti-inflammatory drug
GI	Gastrointestinal
CV	Cardiovascular
NP	Neuropathic pain
CNS	Central nervous system
VGSC	Voltage-gated sodium channel
PNS	Peripheral nervous system
CIP	Congenital insensitivity to pain

PEPD	Paroxysmal extreme pain disorder
IEM	Inherited erythromelalgia
TTX	Tetrodotoxin
DRG	Dorsal root ganglion
STX	Saxitoxin
VSD	Voltage-sensing domain
PD	Pore domain
BTX	Batrachotoxin
VTD	Veratridine
ACT	Aconitine
r	Recombinant
PbTx	Brevetoxins
CTX	Ciguatoxins
LA	Local anaesthetics
SA	Sulphonamides
FLIPR	Fluorescent imaging plate reader
FRET	Fluorescence resonance energy transfer
HTS	High-throughput screening
AAS	Atomic absorption spectroscopy
VIPR	Voltage ion probe reader
STZ	Streptozotocin
CCI	Chronic constriction injury
BID	Twice daily
CFA	Complete Freund's adjuvant
SNL	Spinal nerve ligation
MIA	Monosodium iodoacetate
OA	Osteoarthritis
PSNL	Partial sciatic nerve ligation
MOA	Mechanism of action
OB	Olfactory bulb
fMRI	Functional magnetic resonance imaging
PHN	Postherpetic neuralgia
HV	Healthy volunteer
SD	Single dose
MD	Multiple dose
RBA	Relative bioavailability
DDI	Drug–drug interaction

Conflicts of interest

Both authors are employees of Daiichi Sankyo Co., Ltd.

Notes and references

- 1 A. Fayaz, P. Croft, R. M. Langford, L. J. Donaldson and G. T. Jones, *BMJ Open*, 2012, **6**, e010364; D. J. Gaskin and P. Richard, *J. Pain*, 2012, **13**, 715.
- 2 For a review of analgesic agents, see: C. J. Woolf, *Biol. Psychiatry*, 2020, **87**, 74; S. Obeng, T. Hiranita, F. León, L. R. McMahon and C. R. McCurdy, *J. Med. Chem.*, 2021, **64**, 6523.
- 3 For a review of Na_v1.7 inhibitors, see: J. V. Mulcahy, H. Pajouhesh, J. T. Beckley, A. Delwig, J. D. Bois and J. C. Hunter, *J. Med. Chem.*, 2019, **62**, 8695; M. Alsaloum, G. P. Higerd, P. R. Effraim and S. G. Waxman, *Nat. Rev. Neurol.*, 2020, **16**, 689; M. Kushnarev, I. P. Pirvulescu, K. D. Candido

- and N. N. Knezevic, *Expert Opin. Invest. Drugs*, 2020, **29**, 259; Y. Zhang, K. Wang and Z. Yu, *J. Med. Chem.*, 2020, **63**, 15258.
- O. A. Leon-Casasola, *Am. J. Med.*, 2013, **126**, S3.
 - P. G. Conaghan, A. D. Cook, J. A. Hamilton and P. P. Tak, *Nat. Rev. Rheumatol.*, 2019, **15**, 355; M. C. Osani, E. E. Vaysbrot, M. Zhou, T. E. McAlindon and R. R. Bannuru, *Arthritis Care Res.*, 2020, **72**, 641.
 - U. Alam, G. Sloan and S. Tesfaye, *Drugs*, 2020, **80**, 363; R. Freeman, E. Durso-DeCruz and B. Emir, *Diabetes Care*, 2008, **31**, 1448; C. W. Goodman and A. S. Brett, *N. Engl. J. Med.*, 2017, **377**, 411.
 - M. Mulroy, *Reg. Anesth. Pain Med.*, 2002, **27**, 556.
 - J. J. Cox, F. Reimann, A. K. Nicholas, G. Thornton, E. Roberts, K. Springell, G. Karbani, H. Jafri, J. Mannan, Y. Raashid, L. Al-Gazali, H. Hamamy, E. M. Valente, S. Gorman, R. Williams, D. P. McHale, J. N. Wood, F. M. Gribble and G. C. Woods, *Nature*, 2006, **444**, 894; Y. P. Goldberg, J. MacFarlane, M. L. MacDonald, J. Thompson, M. P. Dube, M. Mattice, R. Fraser, C. Young, S. Hossain, T. Pape, B. Payne, C. Radomski, G. Donaldson, E. Ives, J. Cox, H. B. Youngusband, R. Green, A. Duff, E. Boltshausen, G. A. Grinspan, J. H. Dimon, B. G. Sibley, G. Andria, E. Toscano, J. Kerdraon, D. Bowsheer, S. N. Pimstone, M. E. Samuels, R. Sherrington and M. R. Hayden, *Clin. Genet.*, 2007, **71**, 311; S. Ahmad, L. Dahllund, A. B. Eriksson, D. Hellgren, U. Karlsson, P.-E. Lund, I. A. Meijer, L. Meury, T. Mills, A. Moody, A. Morinville, J. Morten, D. O'Donnell, C. Raynoschek, H. Salter, G. A. Rouleau and J. J. Krupp, *Hum. Mol. Genet.*, 2007, **16**, 2114.
 - J. Weiss, M. Pyrski, E. Jacobi, B. Bufe, V. Willnecker, B. Schick, P. Zizzari, S. J. Gossage, C. A. Greer, T. Leinders-Zufall, C. G. Woods, J. N. Wood and F. Zufall, *Nature*, 2011, **472**, 186.
 - C. R. Furtleman, M. D. Baker, K. A. Parker, S. Moffatt, F. V. Elmslie, B. Abrahamsen, J. Ostman, N. Klugbauer, J. N. Wood, R. M. Gardiner and M. Rees, *Neuron*, 2006, **52**, 767; J. P. Drenth, R. H. M. te Morsche, G. Guillet, A. Taieb, R. L. Kirby and J. B. Jansen, *J. Invest. Dermatol.*, 2005, **124**, 1333; Y. Yang, Y. Wang, S. Li, Z. Xu, H. Li, L. Ma, J. Fan, D. Bu, Z. Fan, G. Wu, J. Jin, B. Ding, X. Zhu and Y. Shen, *J. Med. Genet.*, 2004, **41**, 171; S. D. Dib-Hajj, A. M. Rush, T. R. Cummins, F. M. Hisama, S. Novella and L. Tyrrell, *Brain*, 2005, **128**, 1847.
 - L. Marshall, S. G. Waxman, G. Devigili, R. Eleopra, T. Pierro, R. Lombardi, S. Rinaldo, C. Lettieri, C. G. Faber, I. S. Merkies, S. G. Waxman and G. Lauria, *Pain*, 2014, **155**, 1702.
 - J. Gingras, S. Smith, D. J. Matson, D. Johnson, K. Nye, L. Couture, E. Feric, R. Yin, B. D. Moyer, M. L. Peterson, J. B. Rottman, R. J. Beiler, A. B. Malmberg and S. I. McDonough, *PLoS One*, 2014, **9**, e105895.
 - M. S. Minett, M. A. Nassar, A. K. Clark, G. Passmore, A. H. Dickenson, F. Wang, M. Malcangio and J. N. Wood, *Nat. Commun.*, 2012, **3**, 791; M. S. Minett, S. Falk, S. Santanavarela, Y. D. Bogdanov, M. A. Nassar, A.-M. Heegaard and J. N. Wood, *Cell Rep.*, 2014, **6**, 301.
 - B. Grubinska, L. Chen, M. Alsaloum, N. Rampal, D. J. Matson, C. Yang, K. Taborn, M. Zhang, B. Youngblood, D. Liu, E. Galbreath, S. Allred, M. Lephherd, R. Ferrando, T. J. Kornecook, S. G. Lehto, S. G. Waxman, B. D. Moyer, S. Dib-Hajj and J. Gingras, *Mol. Pain*, 2019, **15**, 1.
 - A. M. Moreno, F. Alemán, G. F. Catroli, M. Hunt, M. Hu, A. Dailamy, A. Pla, S. A. Woller, N. Palmer, U. Parekh, D. McDonald, A. J. Roberts, V. Goodwill, I. Dryden, R. F. Hevner, L. Delay, G. G. dos Santos, T. L. Yaksh and P. Mali, *Sci. Transl. Med.*, 2021, **13**, eaay9056.
 - N. Eijkelkamp, J. E. Linley, M. D. Baker, M. S. Minett, R. Cregg, R. Werdehausen, F. Rugiero and J. N. Wood, *Brain*, 2012, **135**, 2585; W. A. Catterall, A. L. Goldin and S. G. Waxman, *Pharmacol. Rev.*, 2005, **57**, 397.
 - M. H. Meisler and J. A. Kearney, *J. Clin. Invest.*, 2005, **115**, 2010; G. Schmunk and J. J. Gargus, *Front. Genet.*, 2013, **4**, 222.
 - J. A. Black, S. Liu, M. Tanaka, T. R. Cummins and S. G. Waxman, *Pain*, 2004, **108**, 237; B. C. Hains, J. P. Klein, C. Y. Saab, M. J. Craner, J. A. Black and S. G. Waxman, *J. Neurosci.*, 2003, **23**, 8881.
 - C. A. Remme and C. R. Bezzina, *Cardiovasc. Ther.*, 2010, **28**, 287; E. Zaklyazminskaya and S. Dzemeshevich, *Biochim. Biophys. Acta*, 2016, **1863**, 1799.
 - A. Morinville, B. Fundin, L. Meury, A. Jureus, K. Sandberg, J. Krupp, S. Ahmad and D. O'Donnell, *J. Comp. Neurol.*, 2007, **504**, 680; L. Djouhri, R. Newton, S. R. Levinson, C. M. Berry, B. Carruthers and S. N. Lawson, *J. Physiol.*, 2003, **546.2**, 565.
 - B. J. Kerr, V. Souslova, S. B. McMahon and J. N. Wood, *NeuroReport*, 2001, **12**, 3077; C. G. Faber, G. Lauria, I. S. J. Merkies, X. Cheng, C. Han, H.-S. Ahn, A.-K. Persson, J. G. J. Hoeijmakers, M. M. Gerrits, T. Pierro, R. Lombardi, D. Kapetis, S. D. Dib-Hajj and S. G. Waxman, *Proc. Natl. Acad. Sci. U. S. A.*, 2012, **109**, 19444.
 - M. F. Jarvis, P. Honore, C.-C. Shieh, M. Chapman, S. Joshi, X.-F. Zhang, M. Kort, W. Carroll, B. Marron, R. Atkinson, J. Thomas, D. Liu, M. Krambis, Y. Liu, S. McGaraughty, K. Chu, R. Roeloffs, C. Zhong, J. P. Mikusa, G. Hernandez, D. Gauvin, C. Wade, C. Zhu, M. Pai, M. Scanio, L. Shi, I. Drizin, R. Gregg, M. Matulenko, A. Hakeem, M. Gross, M. Johnson, K. Marsh, P. K. Wagoner, J. P. Sullivan, C. R. Faltynek and D. S. Krafte, *Proc. Natl. Acad. Sci. U. S. A.*, 2007, **104**, 8520.
 - M. E. Kort, I. Drizin, R. J. Gregg, M. J. Scanio, L. Shi, M. F. Gross, R. N. Atkinson, M. S. Johnson, G. J. Pacofsky, J. B. Thomas, W. A. Carroll, M. J. Krambis, D. Liu, C. C. Shieh, X. Zhang, G. Hernandez, J. P. Mikusa, C. Zhong, S. Joshi, P. Honore, R. Roeloffs, K. C. Marsh, B. P. Murray, J. Liu, S. Werness, C. R. Faltynek, D. S. Krafte, M. F. Jarvis, M. L. Chapman and B. E. Marron, *J. Med. Chem.*, 2008, **51**, 407; S. K. Bagal, P. J. Bungay, S. M. Denton, K. R. Gibson, M. S. Glossop, T. L. Hay, M. I. Kemp, C. A. L. Lane, M. L. Lewis, G. N. Maw, W. A. Million, C. E. Payne, C. Poinard, D. J. Rawson, B. L. Stammen, E. B. Stevens and L. R. Thompson, *ACS Med. Chem. Lett.*, 2015, **6**, 650.

- 24 S. Pabel, S. Ahmad, P. Tirilomis, T. Stehle, J. Muströph, M. Knierim, N. Dybkova, P. Bengel, A. Holzamer, M. Hilker, K. Streckfuss-Bömeke, G. Hasenfuss, L. S. Maier and S. Sossalla, *Basic Res. Cardiol.*, 2020, **115**, 20.
- 25 D. Julius and A. I. Basbaum, *Nature*, 2001, **413**, 203.
- 26 I. Vetter, J. R. Deuis, A. Mueller, M. R. Israel, H. Starobova, A. Zhang, L. D. Rash and M. Mobli, *Pharmacol. Ther.*, 2017, **172**, 73; S. Noreng, T. Li and J. Payandeh, *J. Mol. Biol.*, 2021, **433**, 166967.
- 27 S. Beaudoin, M. C. Laufer-Sweiler, C. J. Markworth, B. E. Marron, D. S. Millan, D. J. Rawson, S. M. Reister, K. Sasaki, R. I. Storer, P. A. Stuppel, N. A. Swain, C. W. West and S. Zhou, *PCT Int. Appl.*, WO2010079443, Jul 15, 2010.
- 28 J. Payandeh, T. Scheuer, N. Zheng and W. A. Catterall, *Nature*, 2011, **475**, 353.
- 29 S. Ahuja, S. Mukund, L. Deng, K. Khakh, E. Chang, H. Ho, S. Shriver, C. Young, S. Lin, J. P. Johnson Jr., P. Wu, J. Li, M. Coons, C. Tam, B. Brillantes, H. Sampang, K. Mortara, K. K. Bowman, K. R. Clark, A. Estevez, Z. Xie, H. Verschoof, M. Grimwood, C. Dehnhardt, J.-C. Andrez, T. Focken, D. P. Sutherlin, B. S. Safina, M. A. Starovasnik, D. F. Ortwine, Y. Franke, C. J. Cohen, D. H. Hackos, C. M. Koth and J. Payandeh, *Science*, 2015, **350**, aac5464.
- 30 H. Shen, D. Liu, K. Wu, J. Lei and N. Yan, *Science*, 2019, **363**, 1303.
- 31 For a review of structural biology of VGSC, see: S. Cestele and W. A. Catterall, *Biochimie*, 2000, **82**, 883; S. England and M. J. de Groot, *Br. J. Pharmacol.*, 2009, **158**, 1413; M. Stevens, S. Peigneur and J. Tytgat, *Front. Pharmacol.*, 2011, **2**, 1; L. Xu, X. Ding, T. Wang, S. Mou, H. Sun and T. Hou, *Drug Discovery Today*, 2019, **24**, 1389.
- 32 H. A. O'Malley and L. L. Isom, *Annu. Rev. Physiol.*, 2015, **77**, 481.
- 33 S. Bang, J. Yoo, X. Gong, D. Liu, Q. Han, X. Luo, W. Chang, G. Chen, S.-T. Im, Y. H. Kim, J. A. Strong, M.-Z. Zhang, J.-M. Zhang, S.-Y. Lee and R.-R. Ji, *Neurosci. Bull.*, 2018, **34**, 22.
- 34 J. Xu, X. Wang, B. Ensign, M. Li, L. Wu, A. Guia and J. Xu, *Drug Discovery Today*, 2001, **6**, 1278.
- 35 B. T. Priest, A. M. Swensen and O. B. McManus, *Curr. Pharm. Des.*, 2007, **13**, 2325.
- 36 N. Castle, D. Printzenhoff, S. Zellmer, B. Antonio, A. Wickenden and C. Silvia, *Comb. Chem. High Throughput Screening*, 2009, **12**, 107.
- 37 J. P. Felix, B. S. Williams, B. T. Priest, R. M. Brochu, I. E. Dick, V. A. Warren, L. Yan, R. S. Slaughter, G. J. Kaczorowski, M. M. Smith and M. L. Garcia, *Assay Drug Dev. Technol.*, 2004, **2**, 260; E. R. Benjamin, F. Pruthi, S. Olanrewaju, V. I. Ilyin, G. Crumley, E. Kutlina, K. J. Valenzano and R. M. Woodward, *J. Biomol. Screening*, 2006, **11**, 29; Y. Laroche, V. Storme, J. D. Meutter, J. Messens and M. Lauwereys, *Nat. Biotechnol.*, 1994, **12**, 1119.
- 38 S. Trivedi, K. Dekermendjian, R. Julien, J. Huang, P.-E. Lund, J. Krupp, R. Kronqvist, O. Larsson and R. Bostwick, *Assay Drug Dev. Technol.*, 2008, **6**, 167.
- 39 Y. Du, E. Days, I. Romaine, K. K. Abney, K. Kaufmann, G. Sulikowski, S. Stauffer, C. W. Lindsley and C. D. Weaver, *ACS Chem. Neurosci.*, 2015, **6**, 871.
- 40 D. L. Bennett, A. J. Clark, J. Huang, S. G. Waxman and S. D. Dib-Hajj, *Physiol. Rev.*, 2019, **99**, 1079.
- 41 F. Yanagidate and G. R. Strichartz, *Handb. Exp. Pharmacol.*, 2007, vol. 177, p. 95.
- 42 I. W. Glaaser and C. E. Clancy, *Handb. Exp. Pharmacol.*, 2006, vol. 171, p. 99.
- 43 P. Yogeewari, J. V. Ragavendran, R. Thirumurugan, A. Saxena and D. Sriram, *Curr. Drug Targets*, 2004, **5**, 589; A. C. Errington, T. Stöhr and G. Lees, *Curr. Top. Med. Chem.*, 2005, **5**, 15.
- 44 R. Amir, C. E. Argoff, G. J. Bennett, T. R. Cummins, M. E. Durieux, P. Gerner, M. S. Gold, F. Porreca and G. R. Strichartz, *J. Pain*, 2006, **7**, S1.
- 45 T. R. Cummins, P. L. Sheets and S. G. Waxman, *Pain*, 2007, **131**, 243; D. S. Krafft and A. W. Bannon, *Curr. Opin. Pharmacol.*, 2008, **8**, 50.
- 46 C. A. Hinckley, Y. Kuryshv, A. Sers, A. Barre, B. Buisson, H. Naik and M. Hajos, *Mol. Pharmacol.*, 2021, **99**, 49.
- 47 K. Tanaka, S. Suzuki, H. Kobayashi, S. Shibuya, S. Naito, H. Kimoto, Y. Domon, K. Kubota, Y. Kitano, T. Yokoyama, A. Shimizugawa, R. Koishi, D. Asano, K. Takasuna and T. Shinozuka, *Chem. Pharm. Bull.*, 2020, **68**, 653.
- 48 T. Shinozuka, H. Kobayashi, S. Suzuki, K. Tanaka, N. Karanjule, N. Hayashi, T. Tsuda, E. Tokumaru, M. Inoue, K. Ueda, H. Kimoto, Y. Domon, S. Takahashi, K. Kubota, T. Yokoyama, A. Shimizugawa, R. Koishi, D. Asano, T. Sakakura, K. Takasuna, Y. Abe, T. Watanabe and Y. Kitano, *J. Med. Chem.*, 2020, **63**, 10204.
- 49 R. Amir, M. Michaelis and M. Devor, *J. Neurosci.*, 1999, **19**, 8589; C. M. Pedroarena, I. E. Pose, J. Yamuy, M. H. Chase and F. R. Morales, *J. Neurophysiol.*, 1999, **82**, 1465; C. N. Liu, M. Michaelis, R. Amir and M. Devor, *J. Neurophysiol.*, 2000, **84**, 205.
- 50 R. Pal, B. Kumar, J. Akhtar and P. A. Chawla, *Bioorg. Chem.*, 2021, **115**, 105230; S. Bagheri, R. Haddadi, S. Saki, M. Kourosh-Arami and A. Komaki, *Int. J. Dev. Neurosci.*, 2021, **81**, 669.
- 51 P. L. Sheets, C. Heers, T. Stoehr and T. R. Cummins, *J. Pharmacol. Exp. Ther.*, 2008, **326**, 89.
- 52 A. M. Comer and H. M. Lamb, *Drugs*, 2000, **59**, 245; G. Mick and G. Correa-Illanes, *Curr. Med. Res. Opin.*, 2012, **28**, 937.
- 53 E. Perucca, U. Yasothan, G. Clincke and P. Kirkpatrick, *Nat. Rev. Drug Discovery*, 2008, **7**, 973; R. L. Rauck, A. Shaibani, V. Biton, J. Simpson and B. Koch, *Clin. J. Pain*, 2007, **23**, 150.
- 54 B. Beyreuther, N. Callizot and T. Stöhr, *Eur. J. Pharmacol.*, 2006, **539**, 64.
- 55 Y. P. Goldberg, C. J. Cohen, R. Namdari, N. Price, J. A. Cadieux, C. Young, R. Sherrington and S. N. Pimstone, *Pain*, 2014, **155**, 837.
- 56 L. A. McDermott, G. A. Weir, A. C. Themistocleous, A. R. Segerdahl, I. Blesneac, G. Baskozos, A. J. Clark, V. Millar, L. J. Peck, D. Ebner, I. Tracey, J. Serra and D. L. Bennett, *Neuron*, 2019, **101**, 905.
- 57 D. R. Witty, G. Alvaro, D. Derjean, G. M. P. Giblin, K. Gunn, C. Large, D. T. Macpherson, V. Morisset, D. Owen, J.

- Palmer, F. Rugiero, S. Tate, C. A. Hinckley and H. Naik, *ACS Med. Chem. Lett.*, 2020, **11**, 1678.
- 58 J. R. Deuis, J. S. Wingerd, Z. Winter, T. Durek, Z. Dekan, S. R. Sousa, K. Zimmermann, T. Hoffmann, C. Weidner, M. A. Nassar, P. F. Alewood, R. J. Lewis and I. Vetter, *Toxins*, 2016, **8**, 78.
- 59 M. Kotecha, W. P. Cheshire, H. Finnigan, K. Giblin, H. Naik, J. Palmer, S. Tate and J. M. Zakrzewska, *J. Pain Res.*, 2020, **13**, 1601.
- 60 I. Kers, G. Csajernyik, I. Macsari, M. Nylöf, L. Sandberg, K. Skogholm, T. Bueters, A. B. Eriksson, S. Oerther, P.-E. Lund, E. Venyike, J.-E. Nyström and Y. Besidski, *Bioorg. Med. Chem. Lett.*, 2012, **22**, 5618.
- 61 S.-W. Yang, G. D. Ho, D. Tulshian, A. Bercovici, Z. Tan, J. Hanisak, S. Brumfield, J. Matasi, X. Sun, S. A. Sakwa, R. J. Herr, X. Zhou, T. Bridal, M. Urban, J. Vivian, D. Rindgen and S. Sorota, *Bioorg. Med. Chem. Lett.*, 2014, **24**, 4958.
- 62 S. B. Hoyt, C. London, C. Abbadie, J. P. Felix, M. L. Garcia, N. Jochnowitz, B. V. Karanam, X. Li, K. A. Lyons, E. McGowan, B. T. Priest, M. M. Smith, V. A. Warren, B. S. Thomas-Fowlkes, G. J. Kaczorowski and J. L. Duffy, *Bioorg. Med. Chem. Lett.*, 2013, **23**, 3640.
- 63 J. M. Frost, D. A. DeGoey, L. Shi, R. J. Gum, M. M. Fricano, G. L. Lundgaard, O. F. El-Kouhen, G. C. Hsieh, T. Neelands, M. A. Matulenko, J. F. Daanen, M. Pai, N. Ghoreishi-Haack, C. Zhan, X.-F. Zhang and M. E. Kort, *J. Med. Chem.*, 2016, **59**, 3373.
- 64 L. B. Schenkel, E. F. DiMauro, H. N. Nguyen, N. Chakka, B. Du, R. S. Foti, A. Guzman-Perez, M. Jarosh, D. S. La, J. Ligutti, B. C. Milgram, B. D. Moyer, E. A. Peterson, J. Roberts, V. L. Yu and M. M. Weissset, *Bioorg. Med. Chem. Lett.*, 2017, **27**, 3817.
- 65 B. A. Sparling, S. Yi, J. Able, H. Bregman, E. F. DiMauro, R. S. Foti, H. Gao, A. Guzman-Perez, H. Huang, M. Jarosh, T. Kornecook, J. Ligutti, B. C. Milgram, B. D. Moyer, B. Youngblood, V. L. Yub and M. M. Weissa, *Med. Chem. Commun.*, 2017, **8**, 744.
- 66 B. S. Williams, J. P. Felix, B. T. Priest, R. M. Brochu, K. Dai, S. B. Hoyt, C. London, Y. S. Tang, J. L. Duffy, W. H. Parsons, G. J. Kaczorowski and M. L. Garcia, *Biochemistry*, 2007, **46**, 14693.
- 67 S. B. Hoyt, C. London, D. Gorin, M. J. Wyvrat, M. H. Fisher, C. Abbadie, J. P. Felix, M. L. Garcia, X. Li, K. A. Lyons, E. McGowan, D. E. MacIntyre, W. J. Martin, B. T. Priest, A. Ritter, M. M. Smith, V. A. Warren, B. S. Williams, G. J. Kaczorowski and W. H. Parsons, *Bioorg. Med. Chem. Lett.*, 2007, **17**, 4630.
- 68 E. McGowan, S. B. Hoyt, X. Li, K. A. Lyons and C. Abbadie, *Anesth. Analg.*, 2009, **109**, 951.
- 69 I. Macsari, Y. Besidski, G. Csajernyik, L. I. Nilsson, L. Sandberg, U. Yngve, K. Åhlin, T. Bueters, A. B. Eriksson, P.-E. Lund, E. Venyike, S. Oerther, K. H. Blakeman, L. Luo and P. I. Arvidsson, *J. Med. Chem.*, 2012, **55**, 6866.
- 70 H. Bregman, L. Berry, J. L. Buchanan, A. Chen, B. Bingfan Du, E. Feric, M. Hierl, L. Huang, D. Immke, B. Janosky, D. Johnson, X. Li, J. Ligutti, D. Liu, A. Malmberg, D. Matson, J. McDermott, P. Miu, H. N. Nguyen, V. F. Patel, D. Waldon, B. Wilenkin, X. Zheng, A. Zou, S. I. McDonough and E. F. DiMauro, *J. Med. Chem.*, 2011, **54**, 4427.
- 71 D. J. Matson, D. T. Hamamoto, H. Bregman, M. Cooke, D. F. DiMauro, L. Huang, D. Johnson, X. Li, J. McDermott, C. Morgan, B. Wilenkin, A. B. Malmberg, S. I. McDonough and D. A. Simone, *PLoS One*, 2015, **10**, e0138140.
- 72 B. Alrashdi, B. Dawod, A. Schampel, S. Tacke, S. Kuerten, J. S. Marshall and P. D. Côté, *J. Neuroinflammation*, 2019, **16**, 215; R. Ramachandra and K. S. Elmslie, *Mol. Pain*, 2016, **12**, 1.
- 73 N. A. Swain, D. Batchelor, S. Beaudoin, B. M. Bechle, P. A. Bradley, A. D. Brown, B. Brown, K. J. Butcher, R. P. Butt, M. L. Chapman, S. Denton, D. Ellis, S. Galan, S. M. Gaulier, B. S. Greener, M. J. de Groot, M. S. Glossop, I. K. Gurrell, J. Hannam, M. S. Johnson, Z. Lin, C. J. Markworth, B. E. Marron, D. S. Millan, S. Nakagawa, A. Pike, D. Printzenhoff, D. J. Rawson, S. J. Ransley, S. M. Reister, K. Sasaki, R. I. Storer, P. A. Stupple and C. W. West, *J. Med. Chem.*, 2017, **60**, 7029.
- 74 J. W. Theile, M. D. Fuller and M. L. Chapman, *Mol. Pharmacol.*, 2016, **90**, 540.
- 75 A. J. Alexandrou, A. R. Brown, M. L. Chapman, M. Estacion, J. Turner, M. A. Mis, A. Wilbrey, E. C. Payne, A. Gutteridge, P. J. Cox, R. Doyle, D. Printzenhoff, Z. Lin, B. E. Marron, C. West, N. A. Swain, R. I. Storer, P. A. Stupple, N. A. Castle, J. A. Hounshell, M. Rivara, A. Randall, S. D. Dib-Hajj, D. Krafte, S. G. Waxman, M. K. Patel, R. P. Butt and E. B. Stevens, *PLoS One*, 2016, **11**, e0152405.
- 76 K. McCormack, S. Santos, M. L. Chapman, D. S. Krafte, B. E. Marron, C. W. West, M. J. Krambis, B. M. Antonio, S. G. Zellmer, D. Printzenhoff, K. M. Padilla, Z. Lin, P. K. Wagoner, N. A. Swain, P. A. Stupple, M. de Groot, R. P. Butt and N. A. Castle, *Proc. Natl. Acad. Sci. U. S. A.*, 2013, **110**, E2724.
- 77 G. Bankar, S. J. Goodchild, S. Howard, K. Nelkenbrecher, M. Waldbrook, M. Dourado, N. G. Shuart, S. Lin, C. Young, Z. Xie, K. Khakh, E. Chang, L. E. Sojo, A. Lindgren, S. Chowdhury, S. Decker, M. Grimwood, J. Andrez, C. M. Dehnhardt, J. Pang, J. H. Chang, B. S. Safina, D. P. Sutherlin, J. P. Johnson, Jr., D. H. Hackos, C. L. Robinette and C. J. Cohen, *Cell Rep.*, 2018, **24**, 3133.
- 78 B. S. Safina, S. J. McKerrall, S. Sun, C.-A. Chen, S. Chowdhury, Q. Jia, J. Li, A. Y. Zenova, J.-C. Andrez, G. Bankar, P. Bergeron, J. H. Chang, E. Chang, J. Chen, R. Dean, S. M. Decker, A. DiPasquale, T. Focken, I. Hemeon, K. Khakh, A. Kim, R. Kwan, A. Lindgren, S. Lin, J. Maher, J. Mezeyova, D. Misner, K. Nelkenbrecher, J. Pang, R. Reese, S. D. Shields, L. Sojo, T. Sheng, H. Verschoof, M. Waldbrook, M. S. Wilson, Z. Xie, C. Young, T. S. Zabka, D. H. Hackos, D. F. Ortwine, A. D. White, J. P. Johnson, Jr., C. L. Robinette, C. M. Dehnhardt, C. J. Cohen and D. P. Sutherlin, *J. Med. Chem.*, 2021, **64**, 2953.
- 79 T. Focken, S. Liu, N. Chahal, M. Dauphinais, M. E. Grimwood, S. Chowdhury, I. Hemeon, P. Bichler, D.

- Bogucki, M. Waldbrook, G. Bankar, L. E. Sojo, C. Young, S. Lin, N. Shuart, R. Kwan, J. Pang, J. H. Chang, B. S. Safina, D. P. Sutherland, J. P. Johnson, Jr., C. M. Dehnhardt, T. S. Mansour, R. M. Oballa, C. J. Cohen and C. L. Robinette, *ACS Med. Chem. Lett.*, 2016, 7, 277.
- 80 V. Ramdas, R. Talwar, V. Kanoje, R. M. Loriya, M. Banerjee, P. Patil, A. A. Joshi, L. Datrange, A. K. Das, D. S. Walke, V. Kalhapure, T. Khan, G. Gote, U. Dhayagude, S. Deshpande, J. Shaikh, G. Chaure, R. R. Pal, S. Parkale, S. Suravase, S. Bhoskar, R. V. Gupta, A. Kalia, R. Yeshodharan, M. Azhar, J. Daler, V. Mali, G. Sharma, A. Kishore, R. Vyawahare, G. Agarwal, H. Pareek, S. Budhe, A. Nayak, D. Warude, P. K. Gupta, P. Joshi, S. Joshi, S. Darekar, D. Pandey, A. Wagh, P. B. Nigade, M. Mehta, V. Patil, D. Modi, S. Pawar, M. Verma, M. Singh, S. Das, J. Gundu, K. Nemmani, M. G. Bock, S. Sharma, D. Bakhle, R. K. Kamboj and V. P. Palle, *J. Med. Chem.*, 2020, 63, 6107.
- 81 R. F. Graceffa, A. A. Boezio, J. Able, S. Altmann, L. M. Berry, C. Boezio, J. R. Butler, M. Chu-Moyer, M. Cooke, E. F. DiMauro, T. A. Dineen, F. Feric Bojic, R. S. Foti, R. T. Fremeau, Jr., A. Guzman-Perez, H. Gao, H. Gunaydin, H. Huang, L. Huang, C. Ilch, M. Jarosh, T. Kornecook, C. R. Kreiman, D. S. La, J. Ligutti, B. C. Milgram, M.-H. J. Lin, I. E. Marx, H. N. Nguyen, E. A. Peterson, G. Rescourio, J. Roberts, L. Schenkel, R. Shimanovich, B. A. Sparling, J. Stellwagen, K. Taborn, K. R. Vaida, J. Wang, J. Yeoman, V. Yu, D. Zhu, B. D. Moyer and M. M. Weiss, *J. Med. Chem.*, 2017, 60, 5990.
- 82 S. J. McKerrall, T. Nguyen, K. W. Lai, P. Bergeron, L. Deng, A. DiPasquale, J. H. Chang, J. Chen, T. Chernov-Rogan, D. H. Hackos, J. Maher, D. F. Ortwine, J. Pang, J. Payandeh, W. R. Proctor, S. D. Shields, J. Vogt, P. Ji, W. Liu, E. Ballini, L. Schumann, G. Tarozzo, G. Bankar, S. Chowdhury, A. Hasan, J. P. Johnson, Jr., K. Khakh, S. Lin, C. J. Cohen, C. M. Dehnhardt, B. S. Safina and D. P. Sutherland, *J. Med. Chem.*, 2019, 62, 4091.
- 83 D. S. La, E. A. Peterson, C. Bode, A. A. Boezio, H. Bregman, M. Y. Chu-Moyer, J. Coats, E. F. DiMauro, T. A. Dineen, B. Du, H. Gao, R. Graceffa, H. Gunaydin, A. Guzman-Perez, R. Fremeau, Jr., X. Huang, C. Ilch, T. J. Kornecook, C. Kreiman, J. Ligutti, M. H. Jasmine Lin, J. S. McDermott, I. Marx, D. J. Matson, S. I. McDonough, B. D. Moyer, H. N. Nguyen, K. Taborn, V. Yu and M. M. Weiss, *Bioorg. Med. Chem. Lett.*, 2017, 27, 3477.
- 84 J. E. Pero, M. A. Rossi, H. D. G. F. Lehman, M. J. Kelly III, J. J. Mulhearn, S. E. Wolkenberg, M. J. Cato, M. K. Clements, C. J. Daley, T. Filzen, E. N. Finger, Y. Gregan, D. A. Henze, A. Jovanovska, R. Klein, R. L. Kraus, Y. Li, A. Liang, J. M. Majercak, J. Panigel, M. O. Urban, J. Wang, Y. Wang, A. K. Houghton and M. E. Layton, *Bioorg. Med. Chem. Lett.*, 2017, 27, 2683.
- 85 A. J. Roecker, M. Egbertson, K. L. G. Jones, R. Gomez, R. L. Kraus, Y. Li, A. J. Koser, M. O. Urban, R. Klein, M. Clements, J. Panigel, C. Daley, J. Wang, E. N. Finger, J. Majercak, V. Santarelli, I. Gregan, M. Cato, T. Filzen, A. Jovanovska, Y. Wang, D. Wang, L. A. Joyce, E. C. Sherer, X. Peng, X. Wang, H. Sun, P. J. Coleman, A. K. Houghton and M. E. Layton, *Bioorg. Med. Chem. Lett.*, 2017, 27, 2087.
- 86 T. J. Kornecook, R. Yin, S. Altmann, X. Be, V. Berry, C. P. Ilch, M. Jarosh, D. Johnson, J. H. Lee, S. G. Lehto, J. Ligutti, D. Liu, J. Luther, D. Matson, D. Ortuno, J. Roberts, K. Taborn, J. Wang, M. M. Weiss, V. Yu, D. X. D. Zhu, R. T. Fremeau, Jr. and B. D. Moyer, *J. Pharmacol. Exp. Ther.*, 2017, 362, 146.
- 87 I. E. Marx, T. A. Dineen, J. Able, C. Bode, H. Bregman, M. Chu-Moyer, E. F. DiMauro, B. Du, R. S. Foti, R. T. Fremeau, Jr., H. Gao, H. Gunaydin, B. E. Hall, L. Huang, T. Kornecook, C. R. Kreiman, D. S. La, J. Ligutti, M.-H. Lin, S. Liu, J. S. McDermott, B. D. Moyer, E. A. Peterson, J. T. Roberts, P. E. Rose, J. Wang, B. D. Youngblood, V. L. Yu and M. M. Weiss, *ACS Med. Chem. Lett.*, 2016, 7, 1062.
- 88 M. M. Weiss, T. A. Dineen, I. E. Marx, S. Altmann, A. Boezio, H. Bregman, M. Chu-Moyer, E. F. DiMauro, E. F. Bojic, R. S. Foti, H. Gao, R. Graceffa, H. Gunaydin, A. Guzman-Perez, H. Huang, L. Huang, M. Jarosh, T. Kornecook, C. R. Kreiman, J. Ligutti, D. S. La, M.-H. J. Lin, D. Liu, B. D. Moyer, H. N. Nguyen, E. A. Peterson, P. E. Rose, K. Taborn, B. D. Youngblood, V. Yu and R. T. Fremeau, Jr., *J. Med. Chem.*, 2017, 60, 5969.
- 89 R. I. Storer, A. Pike, N. A. Swain, A. J. Alexandrou, B. M. Bechle, D. C. Blakemore, A. D. Brown, N. A. Castle, M. S. Corbett, N. J. Flanagan, D. Fengas, M. S. Johnson, L. H. Jones, B. E. Marron, C. E. Payne, D. Printzenhoff, D. J. Rawson, C. R. Rose, T. Ryckmans, J. Sun, J. W. Theile, R. Torella, E. Tseng and J. S. Warmus, *Bioorg. Med. Chem. Lett.*, 2017, 27, 4805.
- 90 R. L. Kraus, F. Zhao, P. S. Pall, D. Zhou, J. D. Vardigan, A. Danziger, Y. Li, C. Daley, J. E. Ballard, M. K. Clements, R. M. Klein, M. A. Holahan, T. J. Greshock, R. M. Kim, M. E. Layton, C. S. Burgey, J. Serra, D. A. Henze and A. K. Houghton, *Sci. Transl. Med.*, 2021, 13, eaay1050.
- 91 A. J. Roecker, M. E. Layton, J. E. Pero, M. J. Kelly III, T. J. Greshock, R. L. Kraus, Y. Li, R. Klein, M. Clements, C. Daley, A. Jovanovska, J. E. Ballard, D. Wang, F. Zhao, A. P. J. Brunskill, X. Peng, X. Wang, H. Sun, A. K. Houghton and C. S. Burgey, *ACS Med. Chem. Lett.*, 2021, 12, 1038.
- 92 Y.-J. Wu, J. Guernon, J. Shi, J. Ditta, K. J. Robbins, R. Rajamani, A. Easton, A. Newton, C. Bourin, K. Mosure, M. G. Soars, R. J. Knox, M. Matchett, R. L. Pieschl, D. J. Post-Munson, S. Wang, J. Herrington, J. Graef, K. Newberry, L. J. Bristow, N. A. Meanwell, R. Olson, L. A. Thompson and C. Dzierba, *J. Med. Chem.*, 2017, 60, 2513.
- 93 Y.-J. Wua, J. Guernon, A. McClure, G. Luo, R. Rajamani, A. Ng, A. Easton, A. Newton, C. Bourin, D. Parker, K. Mosure, O. Barnaby, M. G. Soars, R. J. Knox, M. Matchett, R. Pieschl, J. Herrington, P. Chen, D. V. Sivarao, L. J. Bristow, N. A. Meanwell, J. Bronson, R. Olson, L. A. Thompson and C. Dzierba, *Bioorg. Med. Chem.*, 2017, 25, 5490.
- 94 G. Luo, L. Chen, A. Easton, A. Newton, C. Bourin, E. Shields, K. Mosure, M. G. Soars, R. J. Knox, M. Matchett, R. L. Pieschl, D. Post-Munson, S. Wang, J. Herrington, J.

- Graef, K. Newberry, D. V. Sivarao, A. Senapati, L. Bristow, N. A. Meanwell, L. A. Thompson and C. D. Dzierba, *J. Med. Chem.*, 2019, **62**, 831.
- 95 A. S. Bell, A. D. Brown, M. J. De Groot, S. M. Gaulier, R. A. Lewthwaite, I. R. Marsh, D. S. Millan, M. Perez Pacheco, D. J. Rawson, N. Sciammetea, R. I. Storer and N. A. Swain, PCT Int. Appl., WO2012007861, Jan 19, 2012.
- 96 D. J. Rawson, R. I. Storer and N. A. Swain, PCT Int. Appl., WO2013088315, Jun 20, 2013.
- 97 A. S. Bell, M. J. De Groot, R. A. Lewthwaite, I. R. Marsh, N. Sciammetta, R. I. Storer and N. A. Swain, PCT Int. Appl., WO 2012095781, July 19, 2012.
- 98 M. E. Rothenberg, M. Tagen, J. H. Chang, J. Boyce-Rustay, M. Friesenhahn, D. H. Hackos, A. Hains, D. Sutherlin, M. Ward and W. Cho, *Clin. Drug Invest.*, 2019, **39**, 873.
- 99 E. F. DiMauro, S. Altmann, L. M. Berry, H. Bregman, N. Chakka, M. Chu-Moyer, E. F. Bojic, R. S. Foti, R. Freneau, H. Gao, H. Gunaydin, A. Guzman-Perez, B. E. Hall, H. Huang, M. Jarosh, T. Kornecook, J. Lee, J. Ligutti, D. Liu, B. D. Moyer, D. Ortuno, P. E. Rose, L. B. Schenkel, K. Taborn, J. Wang, Y. Wang, V. Yu and M. M. Weiss, *J. Med. Chem.*, 2016, **59**, 7818.
- 100 S. Sun, Q. Jia, A. Y. Zenova, M. S. Wilson, S. Chowdhury, T. Focken, J. Li, S. Decker, M. E. Grimwood, J.-C. Andrez, I. Hemeon, T. Sheng, C.-A. Chen, A. White, D. H. Hackos, L. Deng, G. Bankar, K. Khakh, E. Chang, R. Kwan, S. Lin, K. Nelkenbrecher, B. D. Sellers, A. G. DiPasquale, J. Chang, J. Pang, L. Sojo, A. Lindgren, M. Waldbrook, Z. Xie, C. Young, J. P. Johnson, C. L. Robinette, C. J. Cohen, B. S. Safina, D. P. Sutherlin, D. F. Ortwine and C. M. Dehnhardt, *J. Med. Chem.*, 2019, **62**, 908.
- 101 T. Focken, S. Chowdhury, A. Zenova, M. E. Grimwood, C. Chabot, T. Sheng, I. Hemeon, S. M. Decker, M. Wilson, P. Bichler, Q. Jia, S. Sun, C. Young, S. Lin, S. J. Goodchild, N. G. Shuart, E. Chang, Z. Xie, B. Li, K. Khakh, G. Bankar, M. Waldbrook, R. Kwan, K. Nelkenbrecher, P. Karimi Tari, N. Chahal, L. Sojo, C. L. Robinette, A. D. White, C.-A. Chen, Y. Zhang, J. Pang, J. H. Chang, D. H. Hackos, J. P. Johnson, C. J. Cohen, D. F. Ortwine, D. P. Sutherlin, C. M. Dehnhardt and B. S. Safina, *J. Med. Chem.*, 2018, **61**, 4810.
- 102 L. Cao, A. McDonnell, A. Nitzsche, A. Alexandrou, P.-P. Saintot, A. J. C. Loucif, A. R. Brown, G. Young, M. Mis, A. Randall, S. G. Waxman, P. Stanley, S. Kirby, S. Tarabar, A. Gutteridge, R. Butt, R. M. McKernan, P. Whiting, Z. Ali, J. Bilsland and E. B. Stevens, *Sci. Transl. Med.*, 2016, **8**, 335ra56.
- 103 S. Jo and B. P. Bean, *Mol. Pharmacol.*, 2020, **97**, 377.
- 104 D. S. Krafe and R. Roeloffs, PCT Int. Appl., WO2016009303, January 21, 2016.
- 105 Y. Zhang, L. Wang, D. Peng, Q. Zhang, Q. Yang, J. Li, D. Li, D. Tang, M. Chen, S. Liang, Y. Liu, S. Wang and Z. Liu, *J. Biol. Chem.*, 2021, **296**, 100326.
- 106 B. Wu, J. K. Murray, K. L. Andrews, K. Sham, J. Long, J. Aral, J. Ligutti, S. Amagasu, D. Liu, A. Zou, X. Min, Z. Wang, C. P. Ilch, T. J. Kornecook, M.-H. J. Lin, X. Be, L. P. Miranda, B. D. Moyer and K. Biswas, *J. Med. Chem.*, 2018, **61**, 9500.
- 107 K. Biswas, T. E. Nixey, J. K. Murray, J. R. Falsey, L. Yin, H. Liu, J. Gingras, B. E. Hall, B. Herberich, J. R. Holder, H. Li, J. Ligutti, M.-H. J. Lin, D. Liu, B. D. Soriano, M. Soto, L. Tran, C. M. Tegley, A. Zou, K. Gunasekaran, B. D. Moyer, L. Doherty and L. P. Miranda, *ACS Chem. Biol.*, 2017, **12**, 2427.
- 108 M. Kocmalova, M. Kollarik, B. J. Canning, F. Ru, R. A. Herbstsomer, S. Meeker, S. Fonquerna, M. Aparici, M. Miralpeix, X. X. Chi, B. Li, B. Wilenkin, J. McDermott, E. Nisenbaum, J. L. Krajewski and B. J. Udem, *J. Pharmacol. Exp. Ther.*, 2017, **361**, 172.
- 109 L. Yu, K. Tsuji, I. Ujihara, Q. Liu, N. Pavelkova, T. Tsujimura, M. Inoue, S. Meeker, E. Nisenbaum, J. S. McDermott, J. Krajewski, B. J. Udem, M. Kollarik and B. J. Canning, *Eur. J. Pharmacol.*, 2021, **907**, 174192.
- 110 H. Bostock, K. Cikurel and D. Burke, *Muscle Nerve*, 1998, **21**, 137; F. Zhao, M. A. Holahan, A. K. Houghton, R. Hargreaves, J. L. Evelhoch, C. T. Winkelmann and D. S. Williams, *NeuroImage*, 2015, **106**, 364; Å. B. Vallbo, *J. Neurophysiol.*, 2018, **120**, 1415; J. D. Vardigan, A. K. Houghton, H. S. Lange, E. D. Adarayan, P. S. Pall, J. E. Ballard, D. A. Henze and J. M. Uslane, *J. Pain Res.*, 2018, **11**, 735; J. E. Ballard, P. Pall, J. Vardigan, F. Zhao, M. A. Holahan, R. Kraus, Y. Li, D. Henze, A. Houghton, C. S. Burgey and C. Gibson, *Pharm. Res.*, 2020, **37**, 181.
- 111 S. Suzuki, T. Kuroda, H. Kimoto, Y. Domon, K. Kubota, Y. Kitano, T. Yokoyama, A. Shimizugawa, R. Sugita, R. Koishi, D. Asano, K. Tamaki, T. Shinozuka and H. Kobayashi, *Bioorg. Med. Chem. Lett.*, 2015, **25**, 5419.
- 112 G. D. Ho, D. Tulshian, A. Bercovici, Z. Tan, J. Hanisak, S. Brumfield, J. Matasi, C. R. Heap, W. G. Earley, B. Courneya, R. J. Herr, X. Zhou, T. Bridal, D. Rindgen, S. Sorota and S.-W. Yang, *Bioorg. Med. Chem. Lett.*, 2014, **24**, 4110.
- 113 J. M. Zakrzewska, J. Palmer, D. A. Ettlin, M. Obermann, G. M. P. Giblin, V. Morisset, S. Tate and K. Gunn, *Trials*, 2013, **14**, 402.
- 114 J. M. Zakrzewska, J. Palmer, V. Morisset, G. M. P. Giblin, M. Obermann, D. A. Ettlin, G. Cruccu, L. Bendtsen, M. Estacion, D. Derjean, S. G. Waxman, G. Layton, K. Gunn and S. Tate, *Lancet Neurol.*, 2017, **16**, 291.
- 115 Y. P. Goldberg, N. Price, R. Namdari, C. J. Cohen, M. H. Lamers, C. Winters, J. Price, C. E. Young, H. Verschoof, R. Sherrington, S. N. Pimstone and M. R. Hayden, *Pain*, 2012, **153**, 80.
- 116 N. Price, R. Namdari, J. Neville, K. J. W. Proctor, S. Kaber, J. Vest, M. Fetell, R. Malamut, R. P. Sherrington, S. N. Pimstone and Y. P. Goldberg, *Clin. J. Pain*, 2017, **33**, 310.
- 117 H. M. Jones, R. P. Butt, R. W. Webster, I. Gurrell, P. Dzygiel, N. Flanagan, D. Fraier, T. Hay, L. E. Iavarone, J. Luckwell, H. Pearce, A. Phipps, J. Segelbacher, B. Speed and K. Beaumont, *Clin. Pharmacokinet.*, 2016, **55**, 875.
- 118 P. Siebenga, G. van Amerongen, J. L. Hay, A. McDonnell, D. Gorman, R. Butt and G. J. Groeneveld, *Clin. Transl. Sci.*, 2020, **13**, 318.

- 119 A. McDonnell, S. Collins, Z. Ali, L. Iavarone, R. Surujbally, S. Kirby and R. P. Butt, *Pain*, 2018, **159**, 1465.
- 120 Astellas Corporate Web site, <https://www.astellas.com/en/news/7921>, accessed January 2022.
- 121 R. A. Copeland, D. L. Pompliano and T. D. Meek, *Nat. Rev. Drug Discovery*, 2007, **6**, 252.
- 122 M. Flinspach, Q. Xu, A. D. Piekarz, R. Fellows, R. Hagan, A. Gibbs, Y. Liu, R. A. Neff, J. Freedman, W. A. Eckert, M. Zhou, R. Bonesteel, M. W. Pennington, K. A. Eddinger, T. L. Yaksh, M. Hunter, R. V. Swanson and A. D. Wickenden, *Sci. Rep.*, 2017, **7**, 39662.
- 123 D. A. Eagles, C. Y. Chow and G. F. King, *Br. J. Pharmacol.*, 2020, **1**.